JEDEC
STANDARD

Transient Dual Interface Test Method for the Measurement of the Thermal Resistance Junction to Case of Semiconductor Devices with Heat Flow Trough a Single Path

JESD51-14

JEDEC SOLID STATE TECHNOLOGY ASSOCIATION

NOTICE

JEDEC standards and publications contain material that has been prepared, reviewed, and approved through the JEDEC Board of Directors level and subsequently reviewed and approved by the JEDEC legal counsel.

JEDEC standards and publications are designed to serve the public interest through eliminating misunderstandings between manufacturers and purchasers, facilitating interchangeability and improvement of products, and assisting the purchaser in selecting and obtaining with minimum delay the proper product for use by those other than JEDEC members, whether the standard is to be used either domestically or internationally.

JEDEC standards and publications are adopted without regard to whether or not their adoption may involve patents or articles, materials, or processes. By such action JEDEC does not assume any liability to any patent owner, nor does it assume any obligation whatever to parties adopting the JEDEC standards or publications.

The information included in JEDEC standards and publications represents a sound approach to product specification and application, principally from the solid state device manufacturer viewpoint. Within the JEDEC organization there are procedures whereby a JEDEC standard or publication may be further processed and ultimately become an ANSI standard.

No claims to be in conformance with this standard may be made unless all requirements stated in the standard are met.

Inquiries, comments, and suggestions relative to the content of this JEDEC standard or publication should be addressed to JEDEC at the address below, or call (703) 907-7559 or www.jedec.org

Published by
©JEDEC Solid State Technology Association 2010
3103 North 10th Street
Suite 240 South
Arlington, VA 22201-2107

This document may be downloaded free of charge; however JEDEC retains the copyright on this material. By downloading this file the individual agrees not to charge for or resell the resulting material.

PRICE: Please refer to www.jedec.org

TRANSIENT DUAL INTERFACE TEST METHOD FOR THE MEASUREMENT OF THE THERMAL RESISTANCE JUNCTION-TO-CASE OF SEMICONDUCTOR DEVICES WITH HEAT FLOW TROUGH A SINGLE PATH

Contents

Foreword

This document has been prepared by the JEDEC JC-15 Committee on Thermal Characterization. It specifies the details and provisions of a method for the reproducible measurement of the "Junction-to-Case" thermal resistance $R_{\theta JC}$ (θ_{JC}) of semiconductor devices with a one-dimensional conductive heat flow path from the heat dissipating junction of the semiconductor to one case surface of the package. One-dimensional means, that the heat flow direction follows a line. However there is of course heat spreading vertical to that flow direction resulting in a 3-dimensional flow field.

The thermal resistance junction-to-case is one of the most important thermal characteristics of a semiconductor device stating the thermal performance limit under best possible cooling conditions over one package case surface by contacting this surface to a high performance heat sink. $R_{\theta JC}$ should be reported in the data sheet of the device. The lower the value the better is the thermal performance.

Historically the junction-to-case thermal resistance $R_{\theta JC}$ (θ_{JC}) of semiconductor devices has been determined by direct measurement of the temperature difference between junction and the case surface in contact with a water cooled copper heat sink as outlined in MIL Standard 883 [N1]. Since the necessary thermocouple measurement of the case temperature is prone to errors, these results were often not sufficiently reproducible. One problem is a potential temperature distribution at the package case while the thermocouple measures the temperature just at its contact point to the case. This might not be the maximum case temperature. Another reason for a potentially too low case temperature reading is, that thermocouple bead is often not sufficiently insulated against the cold plate and could therefore be cooled from the wire and cold plate side. Further problems arise from considerable clamping pressure to be applied to press the semiconductor device against the heat sink, which closes delaminations. Another source of error is the influence of the drillhole for the thermocouple in the heatsink. This influence increases with smaller devices.

This document specifies a measurement method of the junction-to-case thermal resistance $R_{\theta JC}$ (θ_{JC}) of semiconductor devices without a case temperature measurement by means of a thermocouple at one point. This considerably improves the reproducibility of $R_{\theta JC}$ measurements and allows better comparison of the data and consistent measurements between companies.

The document is an addition to the JESD51 series [N2] of standards for thermal characterization of packaged semiconductor devices. It should be used in conjunction with the electrical test methods described in JEDEC JESD51-1, "Integrated Circuit Thermal Measurement Method - Electrical Test Method (Single Semiconductor Device)" [N3], and document JESD51-12, "Guidelines for Reporting and Using Electronic Package Thermal Information" [N5].

Introduction

The junction-to-case thermal resistance θ_{JC} is a measure of the ability of a semiconductor device to dissipate heat from the surface of the die to a heat sunk package surface. In JESD51-1 [N3] it has been defined as "the thermal resistance from the operating portion of a semiconductor device to the outside surface of the package (case) closest to the chip mounting area when that same surface is properly heat sunk so as to minimize temperature variation across that surface".

The traditional thermocouple measurement as outlined in MIL standard 833 [N1] requires the determination of the junction temperature T_J, the case temperature T_C, and the heating power dissipation P_H, while the device is properly heat-sunk at the case. The junction-to-case thermal resistance is then calculated using

$$\theta_{JC} = \frac{T_J - T_C}{P_H} \tag{1}$$

The result (1) shall be referred to herein as "steady-state θ_{JC}", since it is determined under steady-state conditions and relies on a spatial difference of the temperature along the heat flow path from junction to case. Its measurement involves the difficulty to accurately measure the package case temperature with a thermocouple while that case surface is in close contact with a heat sink. Therefore different measurement set-ups are likely to produce deviant θ_{JC} values.

Contrary to the above, the method described in this document is solely based on transient measurements of the junction temperature, with different cooling conditions at the heat sunk case surface. It does not require the knowledge of the case temperature T_C, thus eliminating all errors involved with its determination. The method relies only on the measurement of the junction temperature. It also does not need high pressure to assure good thermal contact to the heat sink.

Transient Dual Interface (TDI) Measurement Principle and Procedure

The thermal impedance or Zth-function $Z_{\theta JC}(t)$ of a semiconductor device which is heated with constant power P_H starting at time $t = 0$ while its case surface is properly heat-sunk shall be defined as

$$Z_{\theta JC}(t) = \frac{T_J(t) - T_J(t = 0)}{P_H}, \tag{2}$$

i.e., the thermal impedance equals the time-dependent change of the junction temperature $T_J(t)$ divided by the heating power[1]. If the cooling condition at the package case is changed, this should have no influence on the thermal impedance until the temperature starts to increase at the package case where the contact to the heat sink is. A measurement with different contact resistance however changes the total thermal resistance at steady-state and therefore separates the impedance curves of different measurements starting from the point where the external contact resistance contributes, which can be identified as the package case interface.

Two thermal impedance measurements with different contact resistance for cooling the heat sunk package case surface are done to identify this surface in transient measurements. The cumulative thermal resistance at the separation point of these two measurements is defined as $R_{\theta JC}$ (θ_{JC}).

---

[1] When plotted as a diagram, $Z_\theta(t)$ curves are shown in logarithmic time scale. Conversion from linear time scale to logarithmic time scale is relevant from data processing point of view and will be discussed further in detail in the Annexes of this document. When mathematically relevant, linear time and logarithmic time is distinguished by notation t and z respectively, where $z = \ln t$.

TRANSIENT DUAL INTERFACE TEST METHOD FOR THE MEASUREMENT OF THE THERMAL RESISTANCE JUNCTION TO CASE OF SEMICONDUCTOR DEVICES WITH HEAT FLOW TROUGH A SINGLE PATH

(From JEDEC Board Ballot JCB-10-59, formulated under the cognizance of the JC-15 Committee on Thermal Characterization.)

1 Scope

This document specifies a test method (referred to herein as "Transient Dual Interface Measurement") to determine the conductive thermal resistance "Junction-to-Case" $R_{\theta JC}$ (θ_{JC}) of semiconductor devices with a heat flow through a single path, i.e., semiconductor devices with a high conductive heat flow path from the die surface that is heated to a package case surface that can be cooled by contacting it to an external heat sink.

The thermal resistance measured using this document is $R_{\theta JCx}$ or θ_{JCx}, where x denotes the package case side, where the heat is extracted, usually top (x= top) or bottom (x= bot) side.

2 Normative reference

The following normative documents contain provisions that, through reference in this text, constitute provisions of this standard. For dated references, subsequent amendments to, or revisions of, any of these publications do not apply. However, parties to agreements based on this standard are encouraged to investigate the possibility of applying the most recent editions of the normative documents indicated below. For undated references, the latest edition of the normative document referred to applies.

[N1] MIL-STD-883E, METHOD 1012.1, *Thermal Characteristics of Integrated Circuits*, 4 November 1980

[N2] JESD51, *Methodology for the Thermal Measurement of Component Packages (Single Semiconductor Devices)*. This is the overview document for this series of specifications.

[N3] JESD51-1, *Integrated Circuit Thermal Measurement Method - Electrical Test Method*

[N4] JESD51-4, *Thermal Test Chip Guideline (Wire Bond Type Chip)*

[N5] JESD51-12, *Guidelines for Reporting and Using Electronic Package Thermal Information*

[N6] SEMI Test Method #G43-87, *Test Method, Junction-to-Case Thermal Resistance Measurements of Moulded Plastic Packages*

[N7] JESD51-13, *Glossary of thermal measurement terms and definitions*

3 Terms and definitions

For the purposes of this standard, the terms and definitions are given in [N7] JESD51-13, "*Glossary of thermal measurement terms and definitions*" and the following apply:

Further terms and definitions are explained at first occurrence in the text.

4 Junction-to-Case Thermal Resistance Measurement (Test Method)

4.1 Measurement of a transient cooling curve (Thermal Impedance $Z_{\theta JC}$)

4.1.1 Measurement of the junction temperature

The junction temperature T_J of the device under test (DUT) shall be measured as described in document JESD51-1 [N3]. The $Z_{\theta JC}$ curve shall be recorded preferably after the heating power P_H is switched off (cooling curve)[2]. That way the temperature sensitive parameter (TSP) will not be disturbed by the heating voltage or heating current and there is no need to control the heating power during the measurement. This measurement mode can be realized with most product chips as well as thermal test dies. Prior to the measurement of the $Z_{\theta JC}$ curve the TSP of each DUT shall be calibrated individually to account for inter-chip variations of the K-FACTOR, which relates Temperature to the TSP of the device.

Although not recommended, in principle also the heating curve can be used, if constant heating power P_H during the heating pulse time and no electrical cross-talk to a separate TSP device on the chip can be guaranteed[1]. Using the heating curve must be reported with the result data.

4.1.2 Recording the transient cooling curve ($Z_{\theta JC}$)

First a constant heating current I_H shall be applied to the chip of the DUT to heat up the device until thermal steady-state is reached, i.e., until the junction temperature remains constant. If the chip does not provide separate structures for heating and sensing to allow monitoring of the TSP during heating, the temperature can either be monitored in dynamic mode (see JESD51-1) or else the heating time must be chosen long enough as to ensure that steady-state is reached. Since the DUT will be in contact with a water-cooled heat-sink during the measurement (see 4.2) a heating time of 100s will be sufficient in most cases. Control and adjustment of the heating time needed to reach steady state can also be done by test measurements.

Once the hot steady-state has been reached the final heating voltage V_H and heating current I_H are recorded and the heating current is switched off completely or to the level of the measurement current I_M, thus creating a sharp ΔP_H power step. Usually I_M is negligibly small compared to I_H, and the power still supplied by I_M to the DUT is neglected. However the measurement principle just requires a well known step of the heating power, i.e., the power dissipated in the device for heating, and considering the power P_M (caused by the I_M measurement current) is the more general and accurate approach. The higher the heating power step $\Delta P_H = P_H - P_M$ the higher the signal-to-noise ratio (SNR) of the measurement and the more accurate θ_{JC} can be determined.

---

[2] See also remark 2 in 4.1.5

4.1   Measurement of a transient cooling curve (Thermal Impedance $Z_{\theta JC}$) (cont'd)

4.1.2   Recording the transient cooling curve ($Z_{\theta JC}$) (cont'd)

Consequently the heating current should be as high as possible without over-heating the DUT and the P_M power should be kept as small as possible, however, higher I_M current would result in less initial electrical transients (see 4.1.3). The switching signal at $t = 0$ is used to trigger the recording of the TSP signal as a function of time from $t = 0$ to cold steady-state. The sampling rate shall be at least 50 samples per decade of time.

Based on the K-FACTOR of the DUT the recorded TSP values are converted to junction temperatures $T_J(t)$. Figure 1 shows an example of a measured cooling curve. Switching the heating current off at the beginning of the $Z_{\theta JC}$-measurement inevitably causes electrical disturbances of the signal, thus rendering the signal useless for short times. In order to reconstruct the junction temperature T_{J0} at $t = 0$, an "offset-correction" has to be performed (ref. N1).

4.1.3   Offset Correction

Due to the electrical disturbances at the beginning of the measurement, the signal has to be discarded for all points of time t smaller than a certain cut-off time t_{cut}. The temperature change $\Delta T_J(t_{cut})$ within this interval of time can not be neglected. However, for short times t there exists an almost linear relationship between temperature change $\Delta T_J(t)$ and the square-root of time $\sqrt{t}$ that can be used to extrapolate the $T_J(t)$ vs. $\sqrt{t}$ graph to $t = 0$ (Figure 2).
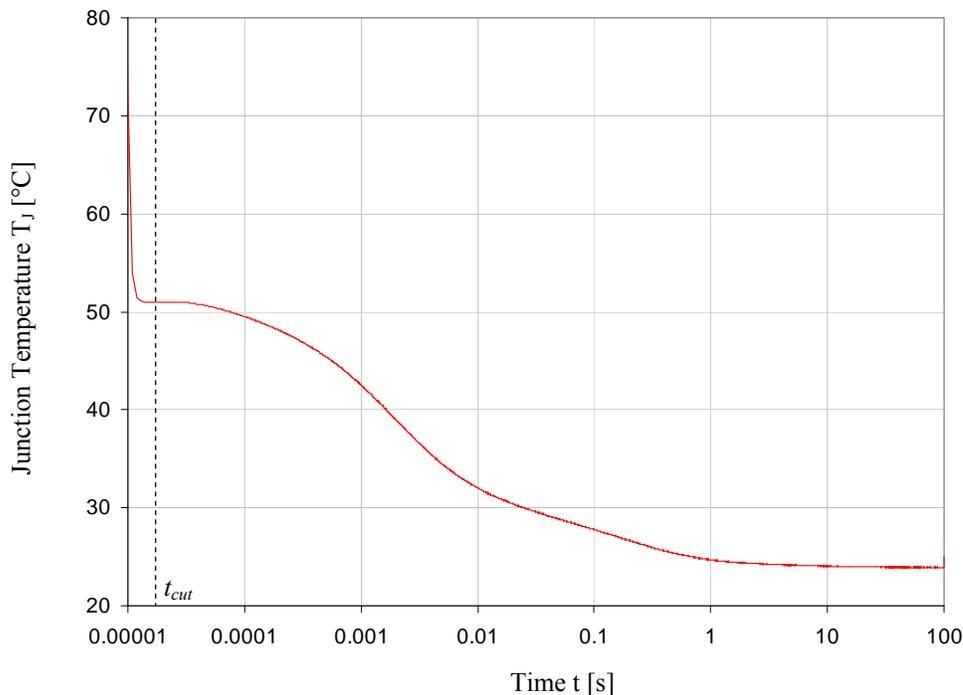

Figure 1 — Semi-logarithmic plot of a measured cooling curve. For short times the signal is disturbed by electrical effects due to switching off the heating current

4.1 Measurement of a transient cooling curve (Thermal Impedance $Z_{\theta JC}$) (cont'd)
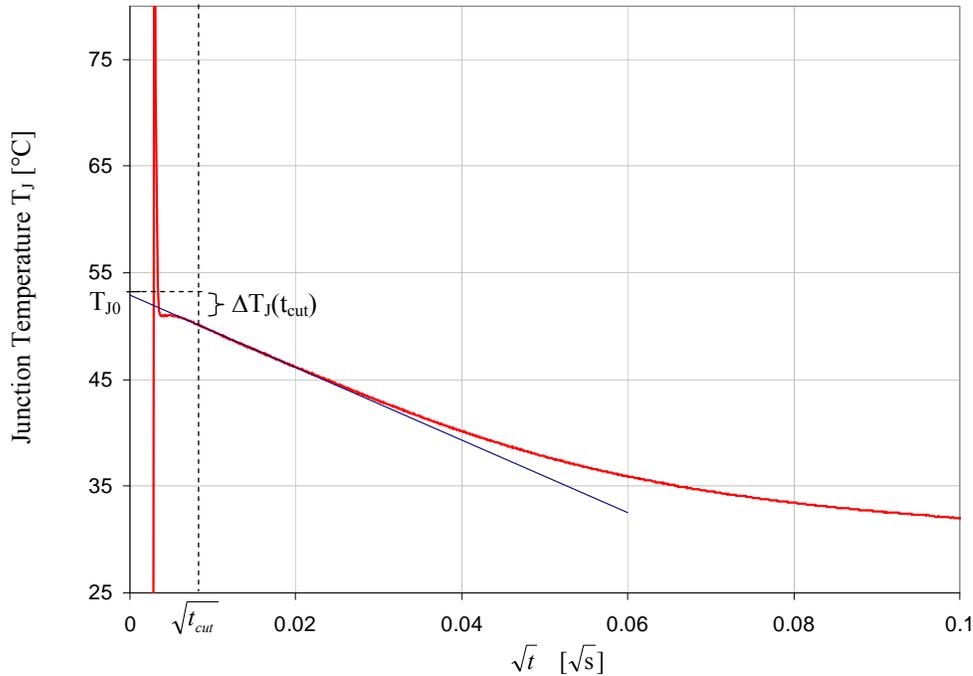
4.1.3 Offset Correction (cont'd)

Figure 2 — Determination of the initial junction temperature $T_{J0} = T_J (t{=}0)$

For a "semi-infinite" plate (i.e., a plate with infinite surface area – ensuring 1-dimensional heat flow perpendicular to the surface – and infinite thickness) of homogeneous material, the surface of which is heated with constant power density P_H/A, it can be shown (see e.g., [1]) that the surface temperature rises/falls linearly with the square root of heating/cooling time when the heating power is switched on/off:

$$\Delta T(t) = \frac{P_H}{A} k_{therm} \sqrt{t} \, , \tag{3}$$

with

$$k_{therm} = \frac{2}{\sqrt{\pi c \rho \lambda}} \, , \tag{4}$$

c, ρ, and λ being the specific heat, density, and thermal conductivity of the plate material, respectively. For short times during which the heat propagation inside the silicon chip is approximately 1-dimensional and undisturbed by boundary effects from the chip bottom surface, the "semi-infinite" plate model can be applied to the heating/cooling of the chip surface. This is confirmed by measurements, as shown in Figure 2. The start temperature T_{J0} can be found by extrapolating the $T_J(t)$ vs. $\sqrt{t}$ graph to $t = 0$. As a side benefit an estimate of the active chip area A can be obtained using equation 3 and the slope m = $\Delta T_J(t_{cut}) / \sqrt{t_{cut}}$ of the linear fit:

$$A = \frac{P}{m} k_{therm} \, . \tag{5}$$

A realistic chip area A calculated this way can serve as cross-check for a reasonable offset correction.

4.1   Measurement of a transient cooling curve (Thermal Impedance $Z_{\theta JC}$) (cont'd)

4.1.4 $Z_{\theta JC}$ curve

The $Z_{\theta JC}$ curve is now computed from the cooling curve $T_J(t)$ using

$$Z_{\theta JC}(t) = \frac{(T_{J0} - T_J(t))}{\Delta P_H} \qquad \text{for } t > t_{cut}. \tag{6}$$

4.1.5   Remarks

1.   The transient thermal impedance $Z_{\theta JC}(t)$ is commonly used to characterize power semi-conductor devices. Measurement equipment to record the cooling curve is usually available.

2.   In case the chip of the DUT provides separate structures for heating the chip and sensing the junction temperature simultaneously (thermal test die) it is also possible to record the heating curve (with constant heating power) instead of the cooling curve. However it must be taken care that the power dissipation P_H remains constant during heating time. The offset correction can be applied analogously, whereas equation 6 has to be replaced by

$$Z_{\theta JC}(t) = \frac{(T_J(t) - T_{J0})}{\Delta P_H} \qquad \text{for } t > t_{cut}. \tag{7}$$

3.   Due to the temperature dependence of material properties, e.g., electrical and thermal conductivity, $Z_{\theta JC}$ curves derived from cooling and heating curves can be slightly different, which might also have an impact on the resulting θ_{JC} value. The main reason is the slight change of dissipated power during heating, which can be avoided by taking the cooling curve as clearly preferred method. Therefore it shall be reported in case the junction-to-case resistance has been determined using the heating curve.

4.2   Transient Dual Interface Measurement Procedure

4.2.1   Measurement principle

The transient dual interface (TDI) measurement requires two $Z_{\theta JC}$ measurements of the same power semiconductor device in contact with a temperature controlled heat-sink. The first measurement (1) shall be performed without any thermal interface material between DUT and cold-plate. For the second measurement (2) a thin layer of thermal grease or oil shall be applied at the interface (Figure 3). The increased interface resistance in case (1) due to the microscopic surface roughness between package and cold-plate ensures a clear separation of the $Z_{\theta JC}$-curves (Figure 4) at some point of time t_S. Since the two $Z_{\theta JC}$ curves start to separate as soon as the heat flow enters the thermal interface layer[3], the $Z_{\theta JC}$-value $Z_{\theta JC}(t_S)$ at this point is close to the steady-state thermal resistance θ_{JC} as defined by equation 1. The splitting point and the progression of the $Z_{\theta JC}$ curves are evaluated to obtain θ_{JC}.

---

[3] This description applies to a heating curve. The cooling response of a device is the complement of the heating response, i.e., both curves result in the same $Z_{\theta JC}$ curve.

4.2 Transient Dual Interface Measurement Procedure (cont'd)

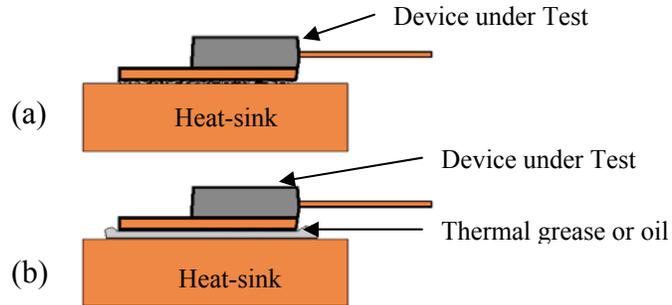### 4.2.1 Measurement principle (cont'd)

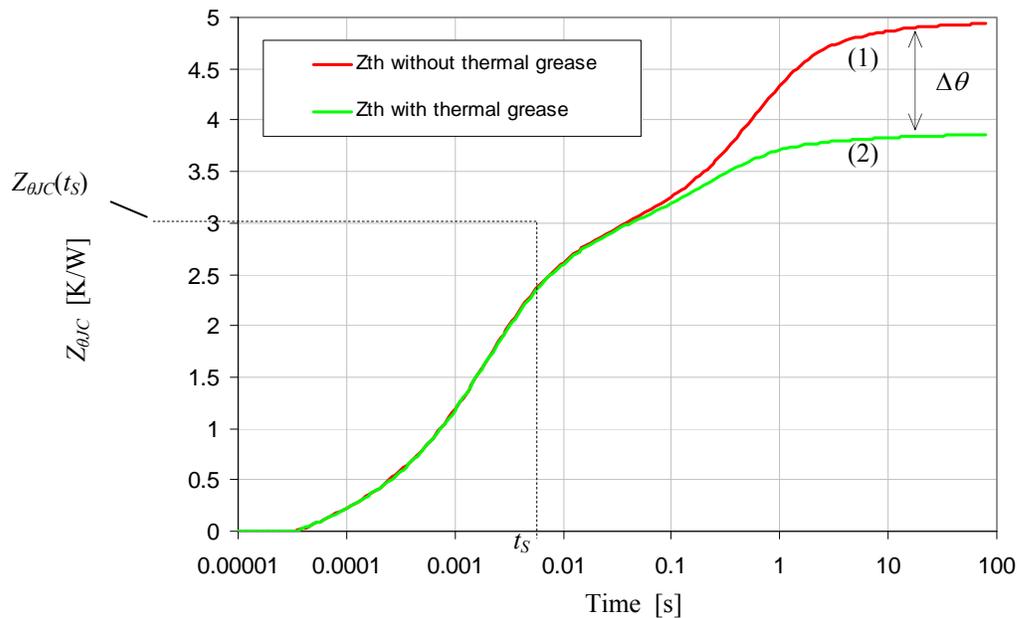**Figure 3 — TDI measurement (a) without and (b) with thermal grease or oil**

Figure 4 — $Z_{\theta JC}$ curves for a TO-263 package measured with (1) and without (2) thermal grease at the interface between heat-slug and cold-plate

4.2.2 Temperature controlled heat-sink

The device under test shall be mounted on a temperature controlled heat sink so that its primary heat removal surface (referred to herein as "case") is in contact with the mounting base. To approximate ideal cooling, the heat sink should be very efficient, i.e., the mounting base shall consist of a copper block, the temperature of which is kept constant by a cooling fluid (usually water) passing through drilled holes in the block. The fluid should flow below the mounting base leaving maximum 2 mm Cu-material between drill hole for water cooling and mounting base surface in contact with the cooled package case surface. A thermostat shall be used to control the temperature of the fluid. The temperature of the fluid T_{Fluid} or of the cold plate T_{CP} shall be measured and reported with the results.

4.2 Transient Dual Interface Measurement Procedure (cont'd)

4.2.2 Temperature controlled heat-sink (cont'd)

Only a moderate pressure shall be applied to press the DUT against the heat-sink. The force shall be strong enough to fasten the device on the mounting base and to ensure good thermal contact between case surface and heat sink. However, too high a pressure will prevent the separation of the two $Z_{\theta JC}$ curves and make their evaluation difficult or impossible. High pressure might also have an undesired influence on θ_{JC} by closing delamination gaps. Therefore the force applied should be in the range of about 10N/cm² which can be realized e.g., by means of a contact pressure spring.

In order to minimize heat flow to the top of the DUT, the clamping bar shall be made of plastic material with a thermal conductivity of $\lambda < 0.5$ W/(m*K) and a thickness of at least 5 mm. A typical heat sink assembly for mounting the device-under test is shown on Figure 5.
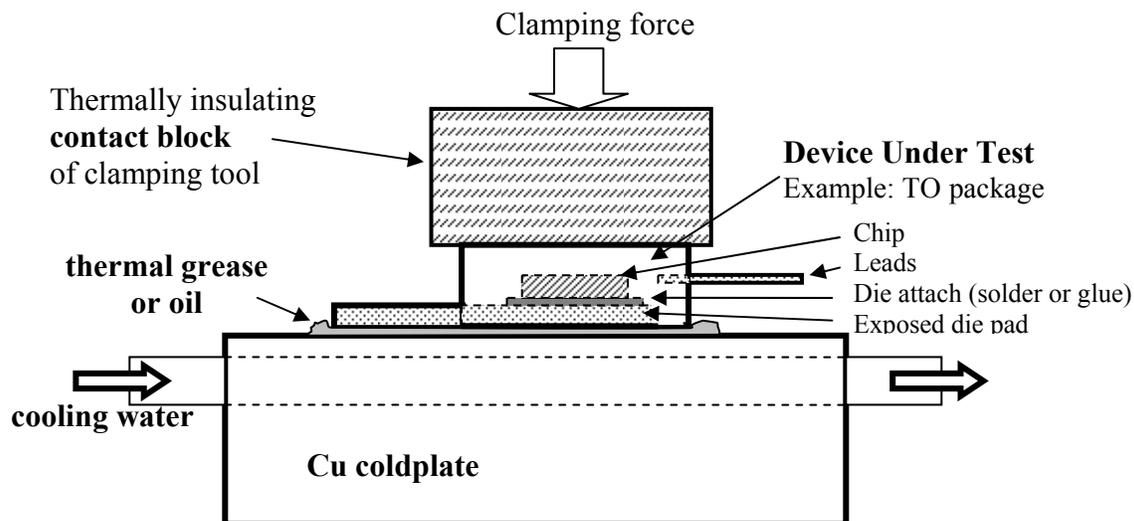
Figure 5 — Schematic of a typical cold-plate set-up

4.2.3 Measurement of $Z_{\theta JC}$ curve (1) without thermal grease or oil

Step 1:   Meticulously clean the contact surfaces of device and heat sink from any adhering material. For the reproducibility of the measurement it is important that neither residues of thermal grease or oil from previous measurements nor any particles trapped in the gap change the thermal contact resistance.

Step 2:   Mount the DUT on the temperature controlled heat sink as described in 4.2.2. Do NOT apply any thermal interface material.

Step 3:   Perform $Z_{\theta JC}$ measurement as described in 4.1.

The resulting $Z_{\theta JC}$-curve is referred to as $Z_{\theta JC1}$.

4.2 Transient Dual Interface Measurement Procedure (cont'd)

4.2.4 Measurement of $Z_{\theta JC}$ curve (2) with thermal grease or oil

Repeat Steps 1-3 in 4.2.3 with modified Step 2:

Step 2: Mount the DUT on the temperature controlled heat sink. This time apply a thin layer of thermal grease or oil at the contact surface of the DUT and heat sink. Make sure that the whole contact surface is coated.

The resulting $Z_{\theta JC}$-curve is referred to as $Z_{\theta JC2}$.

4.2.5 Minimum difference of both $Z_{\theta JC}$-curves at steady state

The minimum difference $\Delta\theta = Z_{\theta JC1} - Z_{\theta JC2}$ at steady state (see Figure 4) is $\Delta\theta \geq 0.5$ K/W.

From experience it turned out, that a smaller difference of the $Z_{\theta JC}$ curves makes it difficult or even impossible to find the separation point of the $Z_{\theta JC}$ curves, because the difference of the $Z_{\theta JC}$ curves is evaluated. This difference should be considerably bigger than the scatter of the measurement points of the $Z_{\theta JC}$-curves.

4.2.6 Remarks

Cold-plates used for θ_{JC} measurements according to the traditional method (see introduction) provide a drilling hole for the thermocouple at the mounting position of the DUT. These cold-plates shall not be used for the test described by this standard unless the drilling hole is shifted away from the mounting position. Otherwise the drilling hole might change the heat flow distribution inside the semiconductor package and therefore the resulting junction-to-case thermal resistance.

5 Evaluation of the Transient Dual Interface Measurement

5.1 Preliminary comments

The $Z_{\theta JC}$-value $Z_{\theta JC}(t_S)$ at the splitting point of curves $Z_{\theta JC1}$ and $Z_{\theta JC2}$ is not necessarily equal to the "steady-state" junction-to-case thermal resistance θ_{JC} defined by equation 1. The reason is that the steady-state (= long time) heat flow distribution inside the device differs from the transient heat flow distribution at time t_S [2].

For power devices with thermally high conductive die attach, $Z_{\theta JC}(t_S)$ is sufficiently close to the "steady-state resistance" to serve as a reliable measure for θ_{JC}. FEM simulations confirm that the deviations to be expected are smaller than the uncertainty inherent to the definition equation 1 of θ_{JC}.

However, if the semiconductor package contains an internal barrier to the heat flow such as thermally low conductive glue, the two $Z_{\theta JC}$ curves can diverge "too early", i.e., $Z_{\theta JC}(t_S) < \theta_{JC}$ [2]. In this case the $Z_{\theta JC}$ curves $Z_{\theta JC1}$ and $Z_{\theta JC2}$ have to be converted to their corresponding structure functions in order to determine the junction-to-case thermal resistance [3]. A more detailed description of structure functions and their computation is provided in Annexes A-C.

5 Evaluation of the Transient Dual Interface Measurement (cont'd)

5.1 Preliminary comments (cont'd)

The structure function represents the distribution of thermal capacitance along the heat flow path, where the position on this path is expressed by the cumulative thermal resistance $R_{\theta\Sigma}$ starting from the junction. Therefore the structure functions of measurement (1) and (2) separate at the point where the heat-flow path changes, which is the case surface of the device under test (Figure 6). The separation point of the structure function indicates the value of θ_{JC}.

While the structure function evaluation method can in principle be applied to all devices with one-dimensional hest flow path irrespective of the die attach, it often fails in practice when applied to devices with very low θ_{JC} [3]. Therefore the application ranges of the two evaluation methods are complementary to some extent: For semiconductor packages with solder die-attach the determination of the splitting point of the $Z_{\theta JC}$ curves is the preferred method, whereas for glue die-attach packages the structure functions shall be evaluated.
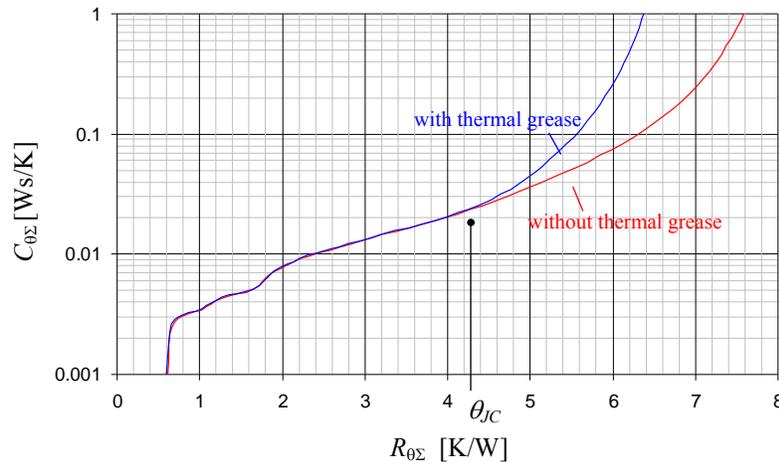

Figure 6 — Cumulative structure functions of a glue die attach device. $C_{\theta\Sigma}$ is the cumulative thermal capacitance along the heat-flow path.

Based on preceding comments the evaluation method shall be chosen as follows:

1. Power semiconductor devices with thermally high conductive die attach, e.g., solder.

   Method 1: Determine the point of separation of $Z_{\theta JC}$ curves $Z_{\theta JC1}$ and $Z_{\theta JC2}$ (see 5.2).

2. Power semiconductor devices with thermally low conductive die attach (most kinds of glue)

   Method 2: Determine the point of separation of the corresponding structure functions (see 5.3).

3. Power semiconductor devices with unknown die attach

   Determine θ_{JC} according to both methods and report the higher value.[4]

For devices with a very small thermal junction-to-case resistance ($\theta_{JC} < 1$ K/W) method 2 often fails. In that case it is safe to assume that method 1 can be applied.[5]

---

[4] In case of thermally high conductive die attach both values should be (approximately) equal. For low conductive die attach the θ_{JC} obtained by method 1 might be too low, therefore report θ_{JC} obtained by method 2 if higher.
[5] If $\theta_{JC} < 1$ K/W according to method 1 it can be safely assumed that there exist no internal heat-flow barriers strong enough to cause a significant deviation of the results of methods 1 and 2.

5   Evaluation of the Transient Dual Interface Measurement (cont'd)

5.2   Method 1: Determination of θ_{JC} based on the point of separation of the $Z_{\theta JC}$ curves

To be applied for semiconductor devices with thermally high conductive die attach, e.g., solder (see 5.1).

5.2.1   Definition of the point of separation

Strictly speaking there is no well defined separation point of the $Z_{\theta JC}$ curves but the gap between the curves widens gradually over some range of time (Figure 7). Therefore it is necessary to define this point of time t_S more precisely.

Regarding the derivates of $Z_{\theta JC1}$ and $Z_{\theta JC2}$ (Figure 8) instead of the original curves is advantageous in several respects:

1. The separation point of the derivatives of the $Z_{\theta JC}$ curves is often better identifiable than is the case with the original curves.

2. Potential errors/deviations of the offset correction (4.1.3) have no influence on the point of separation.

For these reasons the derivatives of the $Z_{\theta JC}$-curves shall be evaluated in order to determine their point of separation. If $z = \ln(t)$ is the logarithmic time, $a(z)$ shall be the $Z_{\theta JC}$-value as a function of z, i.e.,

$$a(z) = Z_{\theta JC}(t = \exp(z)) \text{ for } \qquad z = \ln(t) \tag{8}$$

Figure 11 illustrates the variable transformation $t \to z$. The graph of $a(z)$ on a linear z-scale is congruent with the graph of $Z_{\theta JC}(t)$ on a logarithmic timescale.
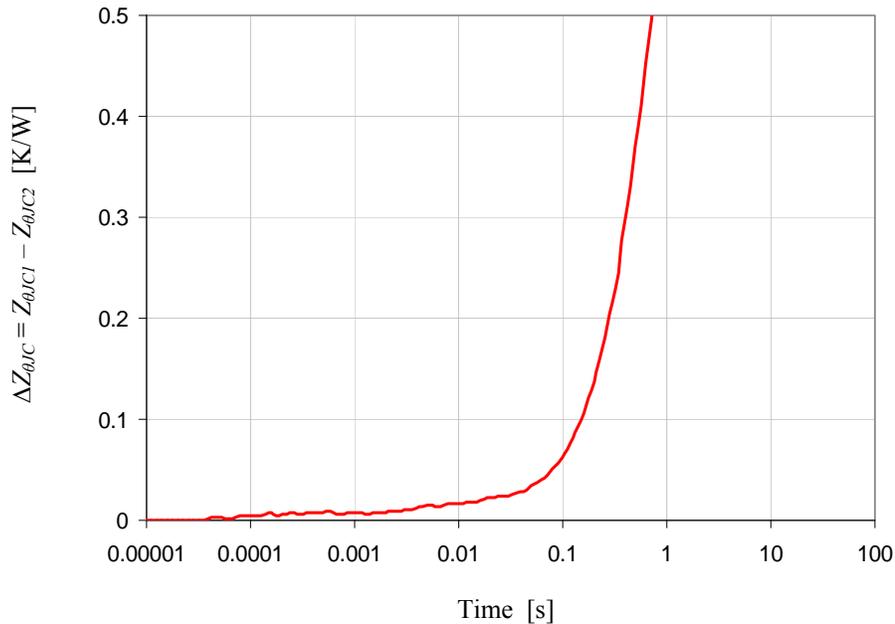

Figure 7 — Difference $\Delta Z_{\theta JC} = Z_{\theta JC1} - Z_{\theta JC2}$ of the two TDI curves from Figure 4.

5.2 **Method 1: Determination of θ_{JC} based on the point of separation of the $Z_{\theta JC}$ curves (cont'd)**

5.2.1 **Definition of the point of separation (cont'd)**

The derivative da/dz is the slope of the $Z_{\theta JC}$-curve plotted with a logarithmic timescale.[6] da_1/dz and da_2/dz shall denote the derivatives of the curves $Z_{\theta JC1}$ and $Z_{\theta JC2}$ (Figure 8).

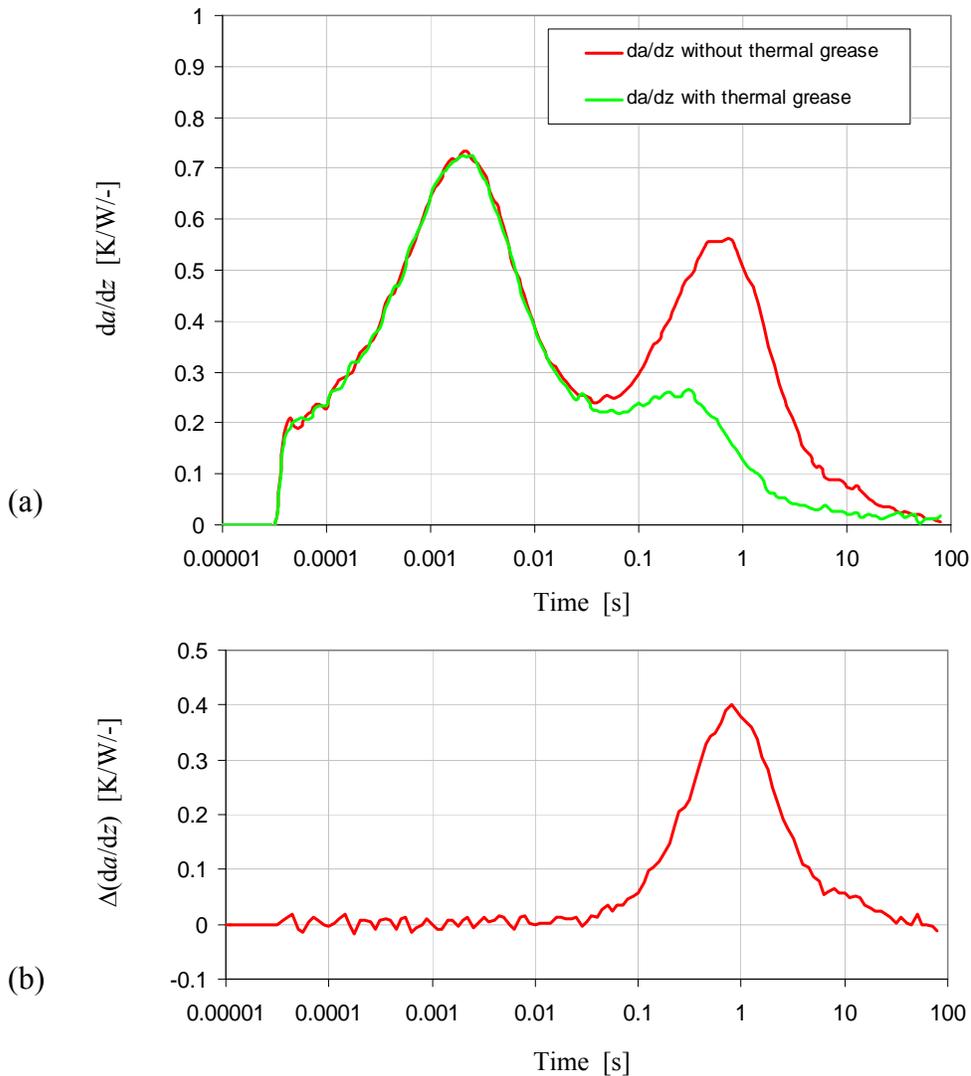**Figure 8 — (a) Derivatives da_1/dt and da_2/dt of the two $Z_{\theta JC}$-curves from Figure 4 and (b) their difference $\Delta(da/dz) = da_1/dz - da_2/dz$.**

---

[6] The derivative da/dz is not to be confused with the derivate $dZ_{\theta JC}/dt$ (the slope of the $Z_{\theta JC}$-curve plotted with a linear timescale). The following relation holds true: $da/dz = t \cdot dZ\theta_{JC}/dt$.

5.2   Method 1: Determination of θ_{JC} based on the point of separation of the $Z_{\theta JC}$ curves (cont'd)
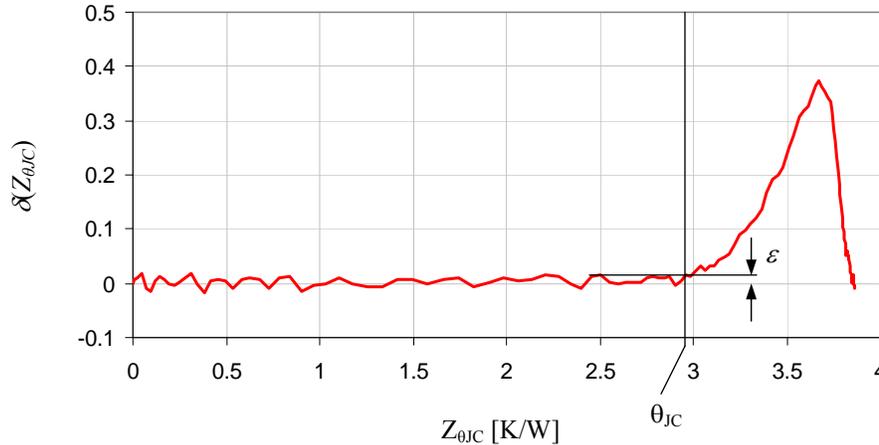
5.2.1   Definition of the point of separation (cont'd)

Figure 9 — Normalized difference $\delta = (\mathrm{d}a_1/\mathrm{d}t - \mathrm{d}a_2/\mathrm{d}t) / \Delta\theta$ plotted against the $Z_{\theta JC}$-value of the thermal grease or oil curve $Z_{\theta JC2}$. This curve is referred to herein as δ-curve

The steady-state distance $\Delta\theta$ of the $Z_{\theta JC}$-curves (see Figure 4) also has an impact on the difference $\Delta(\mathrm{d}a/\mathrm{d}z) = \mathrm{d}a_1/\mathrm{d}z - \mathrm{d}a_2/\mathrm{d}z$ of the derivatives. In order to minimize this influence, $\Delta(\mathrm{d}a/\mathrm{d}z)$ shall be normalized by $\Delta\theta$. The normalized difference shall be plotted against the $Z_{\theta JC}$-value $Z_{\theta JC2}(t)$ of the thermal grease curve (Figure 9) so that θ_{JC} can be taken from this plot directly (Figure 9):

$$\delta(Z_{th2}(t)) = \frac{\Delta(da/dz)(t)}{\Delta\theta} \ . \tag{9}$$

Definition: The point of separation of the $Z_{\theta JC}$-curves $Z_{\theta JC1}$ and $Z_{\theta JC2}$ is the largest time t_S for which the normalized difference $\delta(Z_{\theta JC2}(t_S))$ of the derivatives $\mathrm{d}a_1/\mathrm{d}z$ and $\mathrm{d}a_2/\mathrm{d}z$ is still equal or lower than a certain limit ε.

The junction-to-case thermal resistance θ_{JC} is the $Z_{\theta JC}$-value $Z_{\theta JC2}(t_S)$ of the thermal grease curve at this point of time. It shall be taken from the δ-curve (Figure 9) as the largest $Z_{\theta JC}$-value for which δ is still equal or smaller than the limit ε.

5.2.2   How to choose ε

The θ_{JC} value according to above definition is a function of the limit ε. To be in agreement with the conventional definition of the junction-to-case thermal resistance, the limit ε has to be chosen such that the resulting θ_{JC} is as close as possible to the steady-state resistance as defined by equation 2. Since for real semiconductor devices the actual steady-state θ_{JC} is a priori unknown (and can not be measured accurately enough by means of other methods), one has to rely on finite element simulations to compute the correct ε.

5.2   Method 1: Determination of θ$_{JC}$ based on the point of separation of the Z$_{θJC}$ curves (cont'd)

5.2.2   How to choose ε (cont'd)

Finite element simulations [3] reveal that ε depends on die-size and lead frame geometry. As a general trend, ε is lower for semiconductor devices with small θ_{JC} and higher for devices with high θ_{JC}.
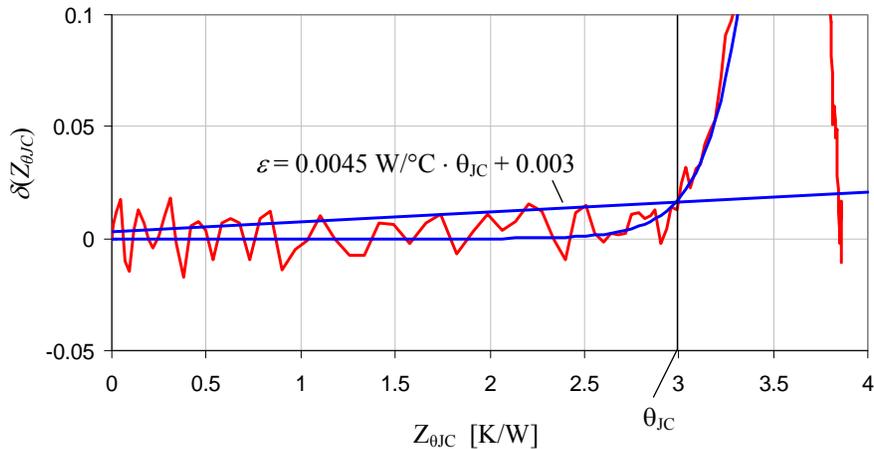

Figure 10 — θ$_{JC}$ is the abscissa of the intersection of δ- and ε-curve

Based on FE simulations with different die-sizes and leadframe geometries the following trend-line has been computed for ε :

$$\varepsilon = 0.0045 \text{ W/K} \cdot \theta_{JC} + 0.003 \tag{10}$$

The junction-to-case thermal resistance θ_{JC} is the abscissa of the intersection point of δ- and ε-curve as shown in Figure 10. In order to prevent that the result is falsified by random fluctuations of the δ-curve, it shall be replaced by an appropriate fit function, e.g., an exponential fit curve

$$\delta = \alpha \cdot \exp(\beta \cdot Z_{\theta JC}) \tag{11}$$

with parameters α and β (Figure 10) optimized for good fitting in the region around θ_{JC} (see 5.2.3, step 4).

5.2.3   Evaluation procedure step by step

It is assumed that the Z$_{θJC}$-curves without (1) and with (2) thermal grease or oil have been measured as described in section 4. The following steps shall be followed to compute the junction-to-case thermal resistance:

Step 1:   Convert the time-values $\{t_1, ..., t_n\}$ (in seconds) of the measurement points to logarithm-mic time $\{z_i = \ln(t_i)\}$. The minimum (maximum) of the logarithmic time-scale is z_{min} (z_{max}).

5.2   Method 1: Determination of θ$_{JC}$ based on the point of separation of the Z$_{\theta JC}$ curves (cont'd)

5.2.3   Evaluation procedure step by step (cont'd)
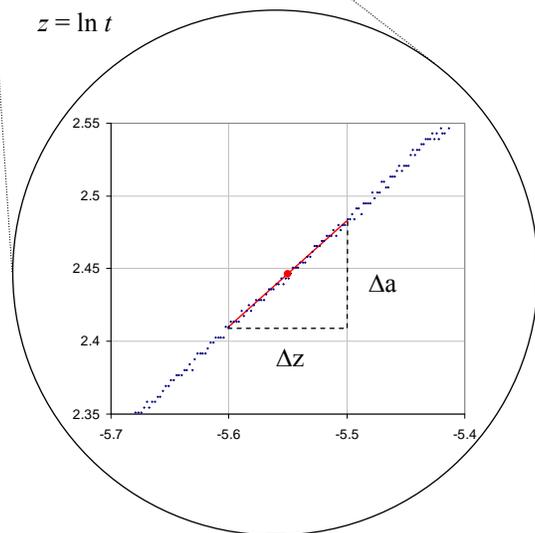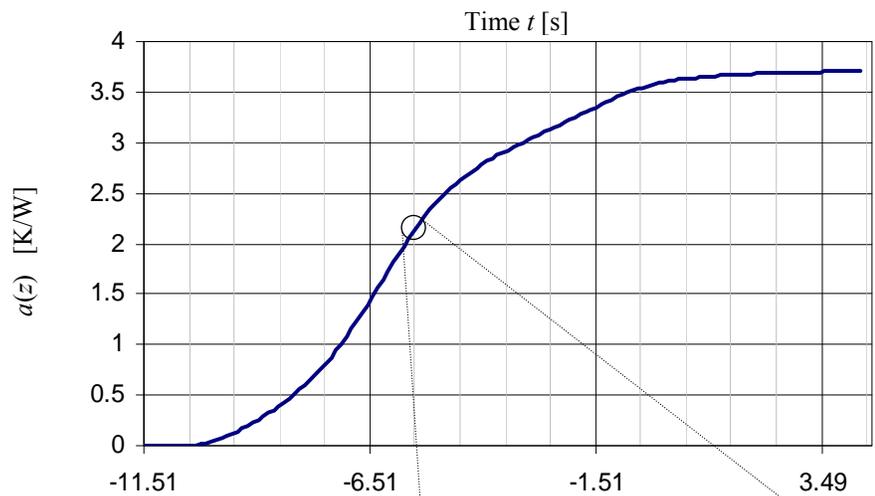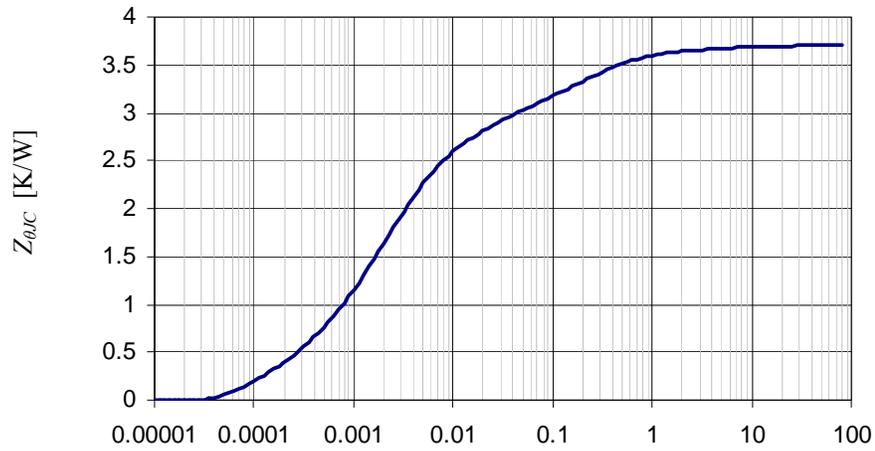
The derivative da/dz (z_j) of the curve $a(z)$ can be approximated by the slope $\Delta a/\Delta z$ of the best fit straight line through the measuring points around z_j.

Figure 11 — Computation of the derivative da/dz from a measured Z$_{\theta JC}$-curve

5.2   Method 1: Determination of θ_{JC} based on the point of separation of the Z_{θJC} curves (cont'd)

5.2.3   Evaluation procedure step by step (cont'd)

Step 2:   Compute the derivatives da_1/dz and da_2/dz. This can be done by piece-wise linear interpolation of the measurement points $\{(z_i, Z_{\theta JC}(t_i))\}_{1/2}$ as shown in Figure 11. In order to compute the difference of da_1/dz and da_2/dz it is important that both derivatives are computed for the same points $\{\tilde{z}_1,...,\tilde{z}_m\}$ which shall be distributed equidistantly in the interval $[z_{min}, z_{max}]$. The number m of interpolation points shall be ≥ 100.

The $Z_{\theta JC}$-values $\{a(\tilde{z}_j)\}$ at the interpolation points are also needed and can be computed using the same piece-wise linear interpolation.

Step 3:   Compute the normalized differences $\delta = (da_1/dz - da_2/dz) / \Delta\theta$ and plot them against the corresponding interpolated $Z_{\theta JC}$-values of the thermal grease curve (Figure 10).

Step 4:   Fit an exponential function $\delta(Z_{\theta JC}) = \alpha \cdot \exp(\beta \cdot Z_{\theta JC})$ to the δ-curve such that the net area enclosed by the graph of the fit-function and the δ-curve in the interval $[0, x]$ is minimized (partial areas must be added up correctly signed). The right interval limit x shall be chosen so that the rising part of the δ-curve is fitted correctly.

Step 5:   The intersection point of the fit function $\delta(Z_{\theta JC}) = \alpha \cdot \exp(\beta \cdot Z_{\theta JC})$ and the ε-curve equation 10 is the junction-to-case thermal resistance θ_{JC}.

5.3   Method 2: Determination of θ_{JC} based on the point of separation of the structure functions

To be applied for semiconductor devices with thermally low conductive die attach (see 5.1)

5.3.1   Preliminary comments

The cumulative structure-function $C_{\theta\Sigma}(R_{\theta\Sigma})$ of a heat-flow path is defined as the cumulative thermal capacitance $C_{\theta\Sigma}$ as a function of the cumulative thermal resistance $R_{\theta\Sigma}$ along this path, starting from the junction. If the heat-flow path is essentially one-dimensional, as is the case for thermally enhanced semiconductor packages with a heat-slug or exposed die-pad, the structure function can provide a map of the heat-flow path which allows identifying partial thermal resistances related to the physical structure. Therefore the structure functions of $Z_{\theta JC}$ measurements (1) and (2) are expected to separate at the point where the heat-flow path changes, which is the case surface of the device under test. The separation point of the cumulative structure function indicates the value of θ_{JC} (Figure 6).

The structure function can be computed from the $Z_{\theta JC}$-curve using dedicated software, e.g., the program TDIM-MASTER which is provided along with this document [4]. This transformation involves several steps (see Annexes A-C). Herein the algorithm can be only briefly outlined. First, the time-constant spectrum $R(z)$ is computed by numerical deconvolution.

5.3 Method 2: Determination of θ_{JC} based on the point of separation of the structure functions (cont'd)

5.3.1 Preliminary comments (cont'd)

If z denotes the logarithmic time $z = \ln(t)$ and $a(z)$ the unit step response as a function of z (see 5.2.1) the following equation holds true:

$$\frac{da}{dz} = R(z) \otimes w(z) \tag{12}$$

with $\quad w(z) = \exp(z - \exp(z))$,

i.e., the time-constant spectrum $R(z)$ can be computed by deconvolution of the time derivative $da(z)/dz$ with the function $w(z)$. By discretization of the time-constant spectrum one obtains a thermally equivalent Foster RC-network which in the next step is transformed into a Cauer RC-network. The cumulative thermal capacitance of the Cauer ladder plotted vs. its cumulative thermal resistance approximates the cumulative structure function. The finer the discretization of the time-constant spectrum, the larger the number of RC-stages, and the better the cumulative structure function is approximated.

From the numerical point of view, deconvolution belongs to the most critical problems. The numerical solution is extremely sensitive to noise in the input data. Therefore a high signal-to-noise ratio (SNR) of the measurement is important. Due to the limited resolution of the deconvolution algorithm, the true structure function can never be reconstructed perfectly from the $Z_{\theta JC}$-curve [5].

The impact of the limited resolution of the deconvolution algorithm used to compute the structure function is less grave for glue die attach devices, simply because their θ_{JC} is larger while the error associated to the evaluation of the structure function is almost independent of θ_{JC} [3]. Therefore the relative error is smaller for glue die attach devices. For devices with a very small θ_{JC} the analysis of the cumulative structure functions is often impeded by numerical effects such as blurring and spurious peaks (Figure 13).

5.3.2 Evaluation procedure step by step

It is assumed that the $Z_{\theta JC}$-curves without (1) and with (2) thermal grease or oil have been measured as described in section 4. The following steps shall be followed to compute the junction-to-case thermal resistance:

Step 1: Convert the $Z_{\theta JC}$-curves $Z_{\theta JC1}$ and $Z_{\theta JC2}$ to the corresponding cumulative structure functions $C_{\theta\Sigma1}$ and $C_{\theta\Sigma2}$ using some dedicated software [4]. A high SNR of the measurements is essential in order to obtain suitable results.

Step 2: Interpolate both structure functions on a common $R_{\theta\Sigma}$ scale and compute the difference $\Delta C_{\theta\Sigma} = C_{\theta\Sigma2} - C_{\theta\Sigma1}$ (Figure 12).

5.3   Method 2: Determination of θ_{JC} based on the point of separation of the structure functions (cont'd)

5.3.2   Evaluation procedure step by step (cont'd)

Step 3:   The junction-to-case thermal resistance θ_{JC} is the point where the difference $\Delta C_{\theta\Sigma}$ clearly starts to rise. If spurious peaks make the determination of θ_{JC} impossible (Figure 12) the $Z_{\theta JC}$-measurements shall be repeated with higher power dissipation in order to achieve a higher SNR.
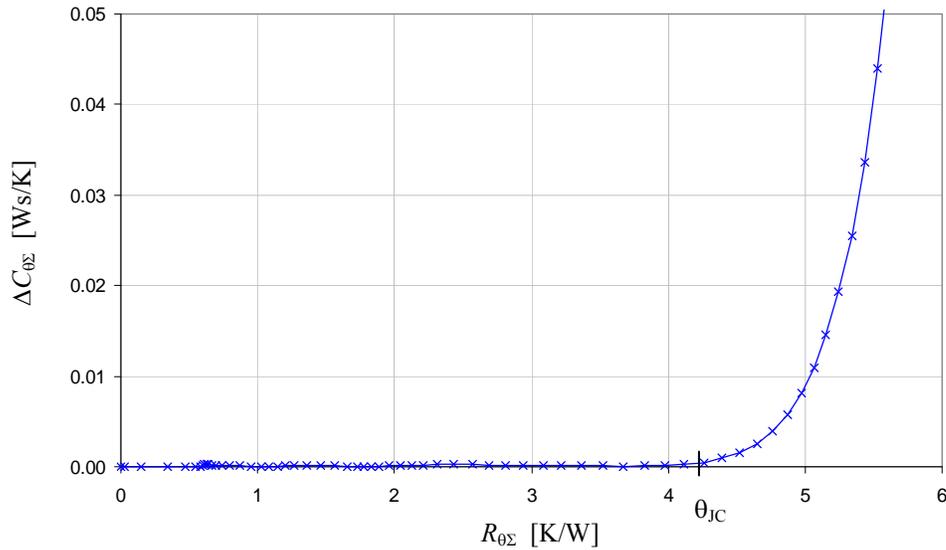
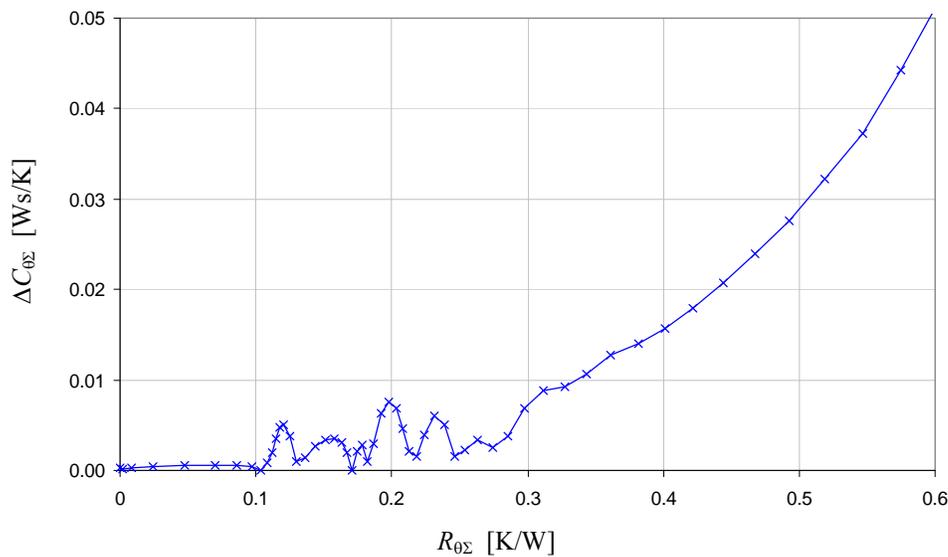**Figure 12 — Difference $\Delta C_{\theta\Sigma}$ of the cumulative structure functions shown in Figure 6.**

Figure 13 — Difference $\Delta C_{\theta\Sigma}$ of the cumulative structure functions for a device with small θ_{JC}.

6   Information to be reported

Together with the measured thermal resistance junction-to-case θ_{JC} the information on all test conditions and data evaluation methods to determine that value must be reported for completeness; refer to Table 1 for information to be supplied with thermal data. The presentation of thermal data or thermal specifications is meaningless without this information.

Table 1 — Information to be supplied with thermal data

Measurement Area	Condition Parameter(s)	Data Parameter(s) and Results
Device Identification		Device Identification Date of Measurements
Device Construction	Refer to appropriate document	Refer to appropriate document
Environmental	Cold plate mounting	T_{CP} or T_{Fluid} [°C] Optional: material, construction, thickness above drill hole, grease / oil, pressure
Measurements	heating method TSP measurement procedure applied power measurement current $Z_{\theta JC}$-curves	e.g., substrate diode e.g., diode voltage cooling / heating curve P_H, I_M $Z_{\theta JC1}, Z_{\theta JC2}$
Data Evaluation	offset correction evaluation method 1 or 2 separation distance	t_{cut}, $\Delta T_J(t_{cut})$ 1: $\Delta da/dz$ or 2: $\Delta C_{\theta\Sigma}$ ε

7   References

1. M. Glavanovics, and M. Zitta, *Thermal Destruction Testing: An Indirect Approach to a Simple Dynamic Model of Smart Power Switches*, Proc. ESSIRC, pp. 236 -239, 2001.

2. D. Schweitzer, *Transient Dual Interface Measurement of the Rth-JC of Power Packages*, Proc. 14th THERMINIC, Rome, pp. 14-19, 2008.

3. D. Schweitzer, H. Pape, R. Kutscherauer, and M. Walder, *How to Evaluate Transient Dual Interface Measurements of the Rth-JC of Power Packages*, Proc. 25th SEMITHERM, San Jose, pp. 172-179, 2009.

4. D. Schweitzer, *Software TDIM-MASTER: Program for the evaluation of transient dual interface measurements of Rth-JC*. This software serves as reference and example implementation of the algorithms described in this standard and can be downloaded from the JEDEC homepage: http://www.jedec.org.

5. D. Schweitzer, H. Pape, and L. Chen, *Transient Measurement of the Junction-to-Case Thermal Resistance Using Structure Functions: Chances and Limits*, Proc. 24th SEMITHERM, San Jose, pp. 193-199, 2008.

Annex A Definition of Time Constant Spectra and Cumulative Structure Functions

A.1   Introduction

In the past decade a new representation for the dynamic thermal behavior of the semiconductor packages has been introduced: the *structure function* [A1]. The purpose of this Annex is to define accurately this function and to present its main characteristics to the extent required for any possible implementation of this standard.

Since structure functions are related closely to the theory of the RC networks and to their different representations, the discussion is started with the notions of time constants, the 'canonic' representations of RC one-ports and the interpretation of the time-constant spectrum. During the discussion we restrict ourselves to the (thermal) RC networks characterized as follows:

- The network is linear and passive
- Driving point behavior is investigated
- Essentially one dimensional heat-flow is assumed

All of these conditions require some explications.

Linearity means that the thermal resistance and capacitance are independent of the temperature itself. In other words: both the thermal conductivity and heat capacity are constant values, without temperature dependence. In reality this theoretical condition is not met exactly but in practical situations it is a reasonable approximation.

Driving point behavior means that the same location of the structure is heated (by e.g., a power step) and measured for its temperature response.

Essentially one dimensional heat flow – besides longitudinal flow – includes more complex heat spreading which with some coordinate system transformation is identical to longitudinal flow in a Cartesian coordinate system. This includes radial spreading in disc-like structures such as an MCPCB of a power LED or in a JEDEC test board, cylindrical spreading or conical spreading. A heat flow path is called essentially 1D path if it is formed as 'series connection' of the regions with the above described heat spreading characteristics which is often the case with real semiconductor device packages. Only the splitting of the heat-flow path poses questions. When the splitting point coincides with the driving point of a main and a parasitic heat-flow path and the total thermal resistance of the parasitic path is known, there is a possibility to eliminate the effect of the parasitic path from the structure function [A11]. Even if such a correction is not possible because the parasitic shunting resistance is not known or the splitting point differs from the driving point, still an 'equivalent' physical structure can be derived, but without direct mapping to the real physical structure in such a case.

A.2   The concept of thermal time-constants

To introduce the time-constant concept, let us consider the example of a little cube with adiabatic sidewalls, attached to an ideal (isothermal) heat-sink. At the top surface a unit power step is applied, uniformly distributed along the surface – see the left hand side of Figure A-1. A very simple thermal model of this cube is a one-stage RC network[7] as shown in the right hand side of the Figure. This can be considered as simple approximate thermal model of a semiconductor device package.
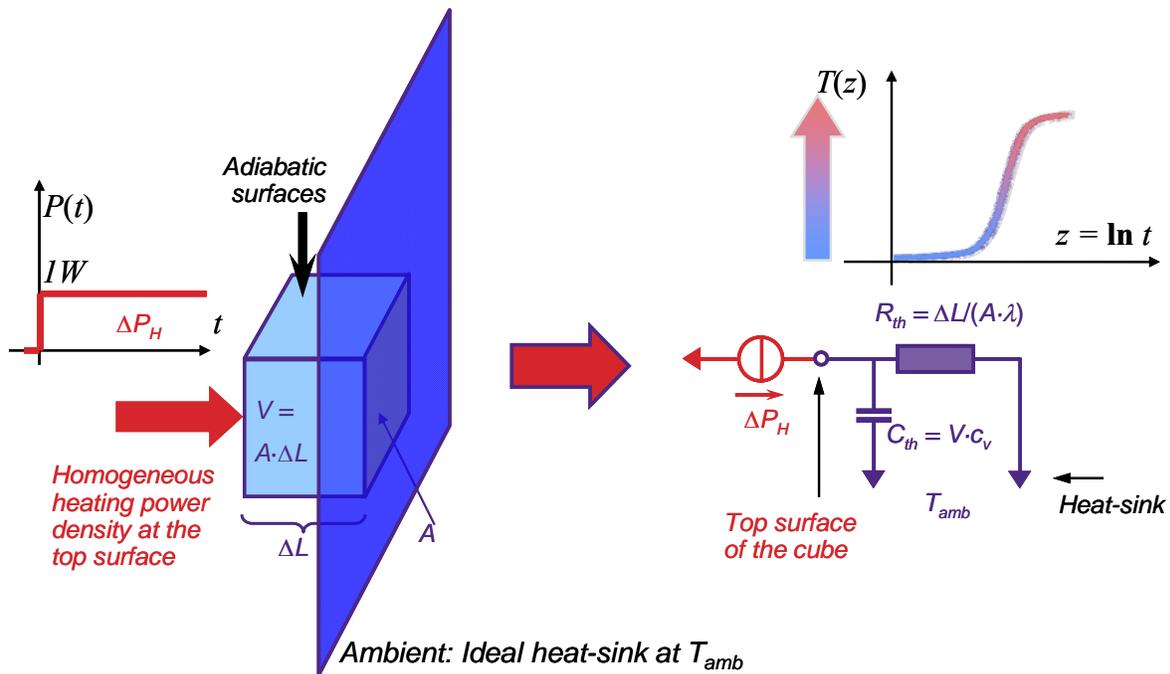

Figure A-1 — Thermal model of a cube with a cross-sectional area of A and a length of ΔL made of a material with a thermal conductivity of λ and a specific heat of c_v
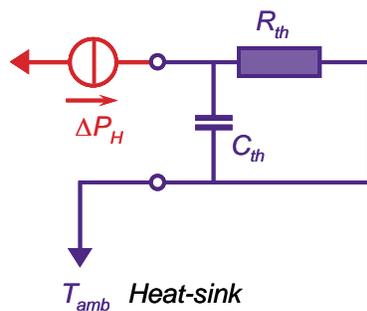

Figure A-2 — A single time-constant RC model

---

[7] The element values of this network model can be calculated from the material properties and the geometry as indicated in Figure A-1.

A.2 The concept of thermal time-constants (cont'd)

In this simplest case the thermal model of a package consists of a thermal resistance and a thermal capacitance. These two elements are connected in parallel as it is shown in Figure A-2. If we apply a ΔP_H power step to this model the temperature will rise following an exponential function

$$T(t) = \Delta P_H \cdot R_{th} \cdot \left[1 - \exp(-t/\tau)\right] \tag{A1}$$

where

$$\tau = R_{th} \cdot C_{th} \tag{A2}$$

is called the *time-constant* of the model.

The model is fully represented by the τ time-constant value and the R_{th} value describing its magnitude. Figure A-3 illustrates this.
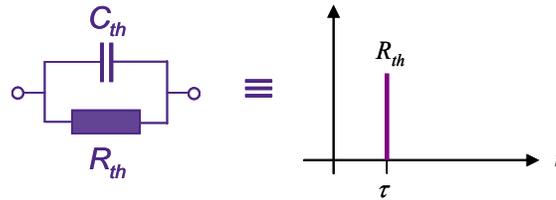

Figure A-3 — The thermal time-constant representation of the model shown in Figure A-2
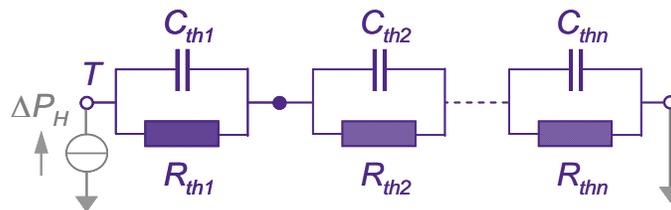

Figure A-4 — An n-stage FOSTER type RC network model of a thermal impedance

The physical structures are usually more complex having several time constants. In this case the temperature response is more precisely represented by the sum of a few exponential functions:

$$T(t) = \Delta P_H \cdot \sum_{i=1}^{n} R_{thi} \cdot \left[1 - \exp(-t/\tau_i)\right] \tag{A3}$$

and the structure is characterized by the n pairs of R_{thi} - τ_i values. It is possible formally to associate a model network to these data; it is shown in Figure A-4. Each pair of R_{thi} thermal resistance and $C_{thi}=\tau_i/R_{thi}$ heat capacitance corresponds to one term in the response of equation A3. The presented structure of the model network is the *FOSTER's normal form*.

The pairs of R_{thi} - τ_i values can be represented in graphical form as well. Figure A-5 shows this representation. The position of the lines along the horizontal axis corresponds to the time-constant whereas their height is proportional to the R_{th} value. This diagram can be regarded as a *discrete spectrum* displaying the time constants occurring in the response and their relative amplitude.

A.2   The concept of thermal time-constants (cont'd)
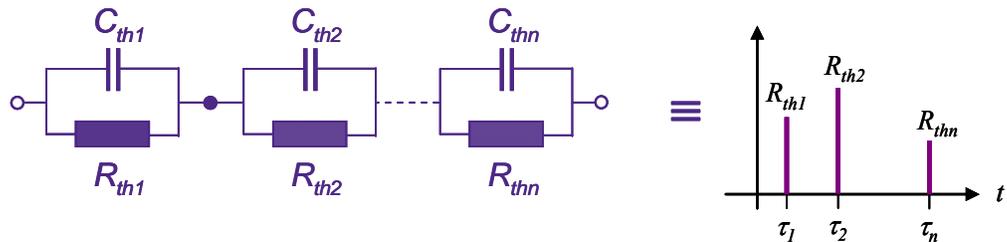
Figure A-5 — The time-constant representation of the n-stage FOSTER type RC network shown in Figure A-4

It would be misleading to associate these thermal resistances and capacitances to the different physical regions of the structure. The FOSTER model is unsuitable to this since it contains node-to-node heat capacitances having no physical reality. An equivalent model exists as well for the RC one-ports: the CAUER network. This model is a ladder network, shown in Figure A-6. This model is excellently matched to the idea of associate the circuit elements with physical regions. This behavior will be the base of the heat-flow path identification by means of structure functions.

Figure A-6 — a) FOSTER type and b) CAUER type representations of the impedance of a thermal one-port

Figure A-7 — In case of distributed parameter RC systems the discrete time-constant values are replaced by the R(τ) time-constant spectrum

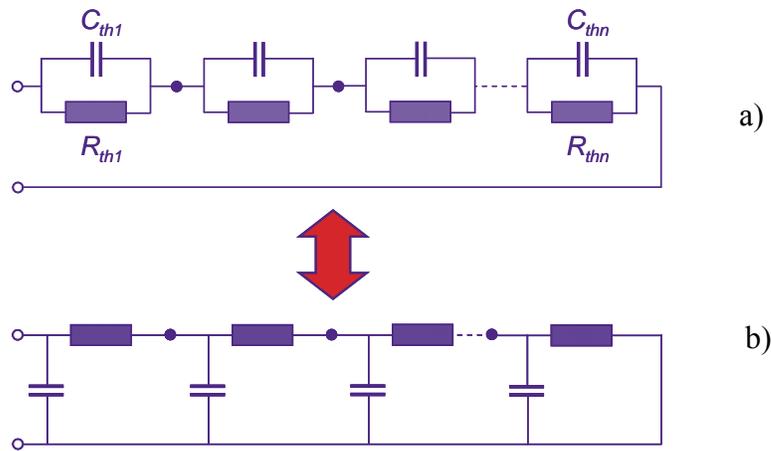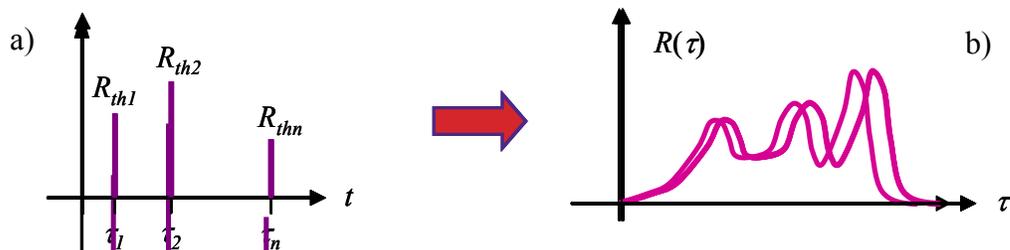## A.2   The concept of thermal time-constants (cont'd)

The FOSTER and the CAUER model are equivalent representations of a RC one-port. Both are *minimal networks* representing the given circuit behavior with the minimum number of components. These models can be transformed one to the other and vice versa. The algorithm of these transformations is described in Annex C.

If the size of the applied power step is $\Delta P_H = 1$ W, the temperature response function (the Z_{th} curve) is also called *unit step response* and is denoted by $a(t)$:

$$a(t) = \sum_{i=1}^{n} R_{thi} \cdot \left[1 - \exp(-t/\tau_i)\right]. \tag{A4}$$

For a real distributed RC system – like thermal systems – the number of stages considered is infinite and the discrete thermal time-constant values are replaced by a continuous spectrum of all possible thermal time constant values (see Figure A-7) as well as summation is replaced by integration in the formula describing the unit-step response function:

$$a(t) = \int_{0}^{\infty} R(\tau)\left[1 - \exp(-t/\tau)\right]d\tau. \tag{A5}$$

where the $R(\tau)$ function is called the *time-constant spectrum*.

A.3   Frequency domain representation of the thermal impedance

The thermal impedance can be calculated as the parallel connection of the R_{th} resistance and $1/sC_{th}$ capacitive impedance (Figure A-2 and Figure A-3). This impedance can be expressed using the time-constant as well:

$$\mathbf{Z(s)} = \frac{R_{th} \cdot 1/\mathbf{s}C_{th}}{R_{th} + 1/\mathbf{s}C_{th}} = \frac{R_{th}}{1 + \mathbf{s}R_{th}C_{th}} = \frac{R_{th}}{1 + \mathbf{s}\tau} \tag{A6}$$

where $\mathbf{s}$ is the so-called *complex frequency*. Substituting $\mathbf{s} = j\omega$ the behavior in the frequency domain is obtained, where ω is the angular frequency of a small sinusoidal (a.c.) signal.

> At the complex frequency of $\mathbf{s} = -1/\tau$ there is a local singularity of the impedance function: $|\mathbf{Z}| \to \infty$. This kind of singularity is called *pole*. The poles of a RC circuit lie always on the negative real axis of the complex $\mathbf{s}$ plane. In the theory of the complex functions a further quantity is associated with a pole: the *residuum* value. This residuum can be very easily calculated in the present case: $Res = R_{th}/\tau$.

The thermal impedance of the system having a finite number of time-constants can be expressed as a sum of members similar to equation A6:

$$\mathbf{Z(s)} = \sum_{i=1}^{n} \frac{R_{thi}}{1 + \mathbf{s}\tau_i} \tag{A7}$$

Figure A-5 and Figure A-6a can help to understand this expression. The algorithm of the conversion between the FOSTER and CAUER canonic networks (see Annex C) is based on this formalism.

A.4   Formal definition of the time-constant spectrum

The pairs of R_{thi} - τ_i values are again shown in Figure A-7a which shows this representation for a finite number of distinct stages of a model network. In the physical structures occurring in the real devices and packages it is impossible to separate the thermal resistances and the thermal capacities. Any infinitesimal cube of the matter shows both resistive and capacitive behavior. The thermal capacitance is distributed along the thermal resistance of the material; this is a *distributed parameter* network [A3].

This distributed structure can be approximated with a model network of very fine web. We divide the structure into a great number of elementary cubes. The sub-network of each cube consists of the heat capacity of the cube and its thermal resistances towards the neighbors. This model is demonstrated in Figure A-8 (for practical reasons only in two dimensions). It is obvious that using a more and more dense mesh of the cubes the model network provides a better and better approximation of the real distributed structure.
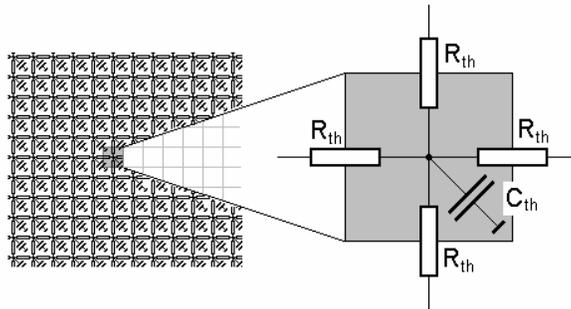
Figure A-8 — A dense lumped network models the distributed property of the matter

This model network has as many time-constants as many lumped capacities[8] it contains. In the spectrum like that shown in Figure A-7a we have a very great number of lines which finally results in continuous spectrum such as the one in Figure A-7b.

Typically the finite-length distributed structures (as a slab of a given material) have discrete time constants but in infinite number. The infinite structures (as the heat conduction path from an IC chip to the ambience) show a continuous spectrum.

In order to present the exact definition of the time-constant spectrum first the logarithmic time-scale will be introduced:

$$z = \ln(t) \ \text{ and } \ \zeta = \ln(\tau) . \tag{A8}$$

The $R(\zeta)$ time-constant function is defined by the following relation:

$$R(\zeta) = \lim_{\Delta\zeta \to 0} \frac{\Sigma \ R_{th} \text{ magnitudes of the time - constants lying between } \zeta \text{ and } \zeta + \Delta\zeta}{\Delta\zeta} . \tag{A9}$$

---

[8] Approximately; it can happen that some time-constants coincide.

A.4   Formal definition of the time-constant spectrum (cont'd)

With equation A9 we have a formal definition of the continuous time-constant spectrum that we introduced intuitively in equation A5 and in Figure A-7b, but in this case in logarithmic scale through the variable transformation according to equation A8. Further data processing relies on this transformation (see e.g., Figure A-9). Linear or logarithmic time is consistently denoted throughout this document by symbols t and z, in case of time-constants by Greek letters τ and ζ, respectively.

> If the complex impedance $\mathbf{Z(s)}$ is known, the time-constant spectrum can be calculated by the following expression [A2]:

$$R(\zeta) = \mp \frac{1}{\pi} \mathrm{Im}\big(\mathbf{Z}(\mathbf{s} = -\exp(-\zeta))\big) \qquad (A10)$$

> Simulations can provide the accurate $\mathbf{Z(s)}$ function. This way the $R(z)$ spectrum can be directly obtained and the structure function and the equivalent physical model can be generated for the simulated structure. Since on the negative real axis of the $\mathbf{s}$ field may lie poles, great precaution should be devoted when applying this equation.

For details of theoretical background on the different kinds of representations of distributed parameter RC networks refer to the technical literature: [A1], [A2], [A7], [A8]

A.5   The structure function

Having the $R(z)$ time-constant spectrum determined there is a rather simple way to draw "heat-flow maps": functions describing the distribution of thermal resistances and capacitances along the path of the heat-flow.

The time-constant spectrum can be considered as the extension of the FOSTER RC model (see Section 2) for the distributed thermal networks. The structure of the lumped element FOSTER model is shown in Figure A-9. In order to construct an approximating lumped element model the $R(z)$ function is split into a number of segments having Δz width. Each Δz segment corresponds to a parallel RC ($R_{th}C_{th}$) circuit, where

$$R_{th} = R(z) \cdot \Delta z \qquad (A11)$$

and

$$C_{th} = \exp(z) / R_{th} . \qquad (A12)$$

If Δz diminishes the number of $R_{th} - C_{th}$ stages increases and the model will be more accurate. Finally, if $\Delta z \rightarrow 0$ the function is transformed to a FOSTER model having infinite number of $R_{th} - C_{th}$ stages connected in series.

The *time-constant spectrum* function is the extension of the FOSTER representation for the continuous (distributed) case. Discretization of the time constant spectrum results in a FOSTER network.
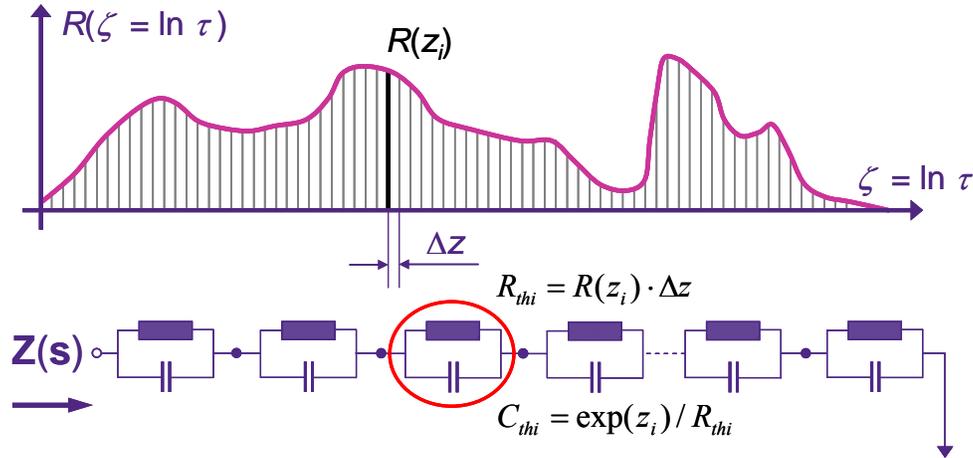
A.5   The structure function (cont'd)

Figure A-9 — Discretized R(z) function and the corresponding FOSTER model

The disadvantage of this FOSTER type of model network is that, although it is a mathematically correct model of the transient behavior, it can not be used for the characterization of the thermal structure, because it contains *node to node* capacitances. The real thermal capacitances are always connected to the datum node of the system (kept at the constant reference temperature) – analogous to the electrical "ground", since the stored thermal energy is proportional to the temperature of *one node*, and not to the temperature difference of two nodes as would be suggested by the FOSTER model. The RC model appropriate for the characterization of thermal structures is the CAUER network. If the FOSTER model is known, the CAUER model can be calculated by using the FOSTER-CAUER transformation described in Annex C.

A.5.1   The cumulative structure function (Protonotarios-Wing function)

In the early paper of PROTONOTARIOS and WING [A4] a function has been introduced which is suitable to describe completely the structure of a non-uniform 1D distributed RC line. This function plots the $C_{\Theta\Sigma}$ *cumulative (thermal) capacitance* as the function of the $R_{\Theta\Sigma}$ *cumulative (thermal) resistance*:

$$C_{\Theta\Sigma}(R_{\Theta\Sigma}) \tag{A13}$$

where

$$C_{\Theta\Sigma} = \int_0^x c_v(\xi)A(\xi)\,d\xi \tag{A14}$$

and

$$R_{\Theta\Sigma} = \int_0^x \frac{1}{\lambda(\xi)}\frac{1}{A(\xi)}d\xi \ , \tag{A15}$$

where c_v is the volumetric heat capacitance, λ is the thermal conductivity, $A(x)$ is the cross-sectional area of the line. The x=0 basis is usually the driving point of the line. This representation provides remarkable advantages like the highly descriptive nature. The function $C_{\Theta\Sigma}(R_{\Theta\Sigma})$ is referred to as the *cumulative structure function* or PROTONOTARIOS-WING function.

A.5.1   The cumulative structure function (Protonotarios-Wing function) (cont'd)

If the distributed RC structure is divided into a great number of elementary Δx slices along the x axis, and each slice is modeled by a serial resistance and a shunt capacitance, a very long CAUER ladder is obtained as the discretized, lumped model of the distributed structure. If $\Delta x \rightarrow 0$, the number of stages in the CAUER network tends to the infinite. The cumulative structure function defines directly this infinite CAUER ladder as shown in Figure A-8.

In other words: the cumulative structure function is the extension of the CAUER ladder description for the continuous (distributed) case. Discretization of the cumulative structure function results in a CAUER network.
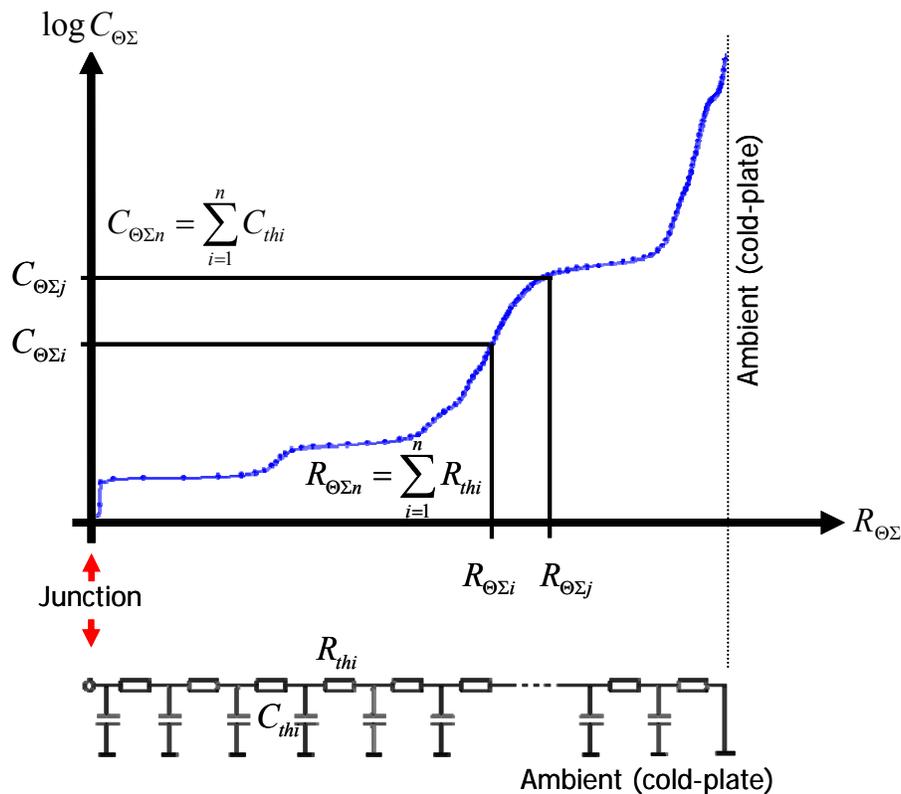
Figure A-10 — The cumulative structure function and the CAUER ladder model

A.5.2   How to construct the cumulative structure function in practice?

Now we have to answer the following question: how to get the cumulative structure function? For practical purposes an approximate way is suitable. As it was demonstrated in Figure A-9 the lumped element FOSTER model can be generated from the $R(z)$ spectrum. (Annex B describes how to obtain time-constant spectra from Z_{th} curves.) By using the FOSTER$\rightarrow$CAUER transformation (Annex C), this model can be turned into a CAUER ladder. As it is shown in Figure A-10 this ladder is a discretized approximation of the cumulative structure function (also known as PROTONOTARIUS-WING function).

The cumulative thermal capacitance of packaged semiconductor devices varies in a wide range of order of magnitude, therefore their cumulative structure functions are typically plotted in lin-log scale as also shown in Figure A-10.

A.6   References

[A1]   V. Székely, Tran van Bien: "Fine structure of heat flow path in semiconductor devices: a measurement and identification method", Solid-State Electronics 31(9): 1363-1368 (1988)

[A2]   V. Székely: "On the representation of infinite-length distributed RC one-ports", *IEEE Transactions on Circuits and Systems II – Analog and Digital Signal Processing*, **38**(7):711–719, 1991.

[A3]   M.S.Ghausi and J.J.Kelly: "Introduction to Distributed Parameter Networks", New York: Holt, Rinehart and Winston, 1968

[A4]   E. N. Protonotarios, O. Wing: "Theory of nonuniform RC lines", *IEEE Transactions on Circuit Theory*, **14**(1):2-12 (1967)

[A5]   V. Székely: "A New Evaluation Method of Thermal Transient Measurement Results", *Microelectronics Journal*, Vol. **28**(3): 277-292 (1997)

[A6]   V. Székely: "Identification of RC Networks by Deconvolution: Chances and Limits", *IEEE Transactions on Circuits and Systems I – Fundamental Theory and Applications,* **45**(3): 244-258. (1998)

[A7]   V. Székely: "Distributed RC networks" In: Wai-Kai Chen (ed.): The Circuits and Filters Handbook, Boca Raton: CRC Press Inc., 2003. pp. 1201-1222. (The electrical engineering handbook series) ISBN:0-8493-0912-3

[A8]   V. Székely, M. Rencz: "Thermal Dynamics and the Time Constant Domain", *IEEE Transactions On Components and Packaging Technologies*, **23**(3): 687-594 (2000)

[A9]   T. J. Kennett, W. V. Prestwich: "On the Deconvolution of Exponential Response Functions", *Phys. Med. Biol.* **24**(6): 1107-1122 (1979)

[A10]   V. Székely, M. Rencz, A. Poppe, B. Courtois: "THERMODEL: a tool for thermal model generation, and application for MEMS" Analog Integrated Circuits and Signal Processing 29(1-2): 49-59 (2001)

[A11]   M. Rencz, A. Poppe, E. Kollár, S. Ress, V. Székely: "Increasing the Accuracy of Structure Function Based Thermal Material Parameter Measurements", *IEEE Transactions On Components and Packaging Technologies* **28**(1): 51-57 (2005)

Annex B Obtaining time-constant spectra from Z_{th} functions

There is a close relation between the time-constant spectrum and the time response of the thermal system, i.e., in this case the Z_{th}-curves. In fact Z_{th} curves are equivalent to unit step response functions introduced by equation A5 except that instead of linear time used in equation A5 time is in logarithmic scale. If $a(z)$ denotes the Z_{th}-value as function of logarithmic time z, i.e.,

$$a(z) = Z_{th}(t=\exp(z)) \text{ for } z = \ln(t),$$ (B1)

it can be proven (see references [A1] and [A7] in Annex A) that the following relationship holds between the $a(z)$ unit-step thermal response function (i.e., the Z_{th} curve) and the $R(\zeta)$ time-constant spectrum[9]:

$$\frac{d}{dz} a(z) = \int_0^\infty R(\zeta)[\exp(z - \zeta - \exp(z - \zeta))]d\zeta .$$ (B2)

Introducing the

$$w_z(z) = \exp[z - \exp(z)]$$ (B3)

notation equation A5 can be rewritten as

$$\frac{d}{dz} a(z) = \int_0^\infty R(\zeta) \cdot w_z(z - \zeta)d\zeta .$$ (B4)

It can be realized that the right hand side of equation B4 is a *convolution integral*[10]. Using the $\otimes$ symbol for the convolution operation the relationship between the unit-step thermal response (Z_{th} curve) and the thermal time-constant spectrum can be written as

$$\frac{d}{dz} a(z) = R(z) \otimes w_z(z) .$$ (B5)

The $w_z(z)$ function is a fixed, known function – see formula (B3) – and the $a(z)$ function (Z_{th} curve) can be measured (e.g., with the electrical test method), therefore the $R(z)$ thermal time-constant spectrum can be calculated with the help of *deconvolution*[5], the inverse operation of the convolution:

$$R(z) = \left[\frac{d}{dz} a(z) \right] \otimes^{-1} w_z(z)$$ (B6)

where the $\otimes^{-1}$ symbol represents the deconvolution operation.

Different deconvolution algorithms have been applied successfully to perform this operation, among them *Bayesian deconvolution* and *Fourier-domain inverse filtering*. The latter algorithm, also known as *Frequency domain deconvolution*, shall be described herein more closely.

---

[9] Equation B2 is obtained from equation A5 after the $t=\exp(z)$ substitution, equivalent transformations and derivation with respect to variable z are applied.

[10] *Convolution* and *deconvolution* are common operations in signal processing. Two dimensional versions of these operations are extensively used e.g., in image processing to enhance images.

Annex B Obtaining time-constant spectra from Z_{th} functions (cont'd)

Computing the Fourier transform of both sides of equation B5 one obtains

$$M(\Phi) = V(\Phi) \cdot W(\Phi) \tag{B7}$$

with the generalized frequency Φ and the Fourier transforms $M(\Phi)$, $V(\Phi)$, and $W(\Phi)$ of da/dz, $R(z)$, and $w(z)$, respectively. It should be noted that Φ is not a frequency in the usual sense since the variable z in equation A10 denotes not time but logarithmic time.

In Fourier domain the convolution equation B5 becomes a simple multiplication. With that knowledge the computation of the time constant spectrum $R(z)$ seems to be quite straight-forward: Compute $V(\Phi)$ by a division $V(\Phi) = M(\Phi)/W(\Phi)$ and transform $V(\Phi)$ back into z-domain: $R(z) = F^{-1}(V(\Phi))$. Unfortunately it is not that simple.

There is always some noise $n(z)$ superimposed on the signal da/dz, i.e., the "measured" signal $m^*(z)$ is

$$m^*(z) = \frac{da}{dz} + n(z). \tag{B8}$$

Even if the Z_{th} curve has been obtained by simulation, the quantization errors due to the finite length numerical representation of the numbers constitute a non-negligible noise component. The Fourier transform of the noisy signal $m^*(z)$ becomes

$$M^*(\Phi) = M(\Phi) + N(\Phi) = V^*(\Phi) \cdot W(\Phi), \tag{B9}$$

$N(\Phi)$ being the Fourier transform of $n(z)$. I.e., the noise will also be present in the quotient

$$V^*(\Phi) = \frac{M^*(\Phi)}{W(\Phi)} = \frac{M(\Phi)}{W(\Phi)} + \frac{N(\Phi)}{W(\Phi)} \tag{B10}$$

The higher frequency components of $W(\Phi)$ are extremely small, whereas the noise spectrum contains mainly high-frequency components. Therefore the division $N(\Phi)/W(\Phi)$ in equation B10 extremely enhances the noise in $V^*(\Phi)$. Figure B-1 shows an example of the power spectrum $|M^*(\Phi)|^2$ obtained for a Z_{th} measurement along with the power spectrum $|W(\Phi)|^2$. It can be seen that $|W(\Phi)|^2$ vanishes very quickly for higher frequencies Φ, whereas the amplitude of the noise component of $|M^*(\Phi)|^2$ remains more or less constant. Without further measures to reduce the noise in $V^*(\Phi)$ the back-transform $F^{-1}(V^*(\Phi))$ would not even remotely resemble the desired time constant spectrum.

Annex B Obtaining time-constant spectra from Z_{th} functions (cont'd)
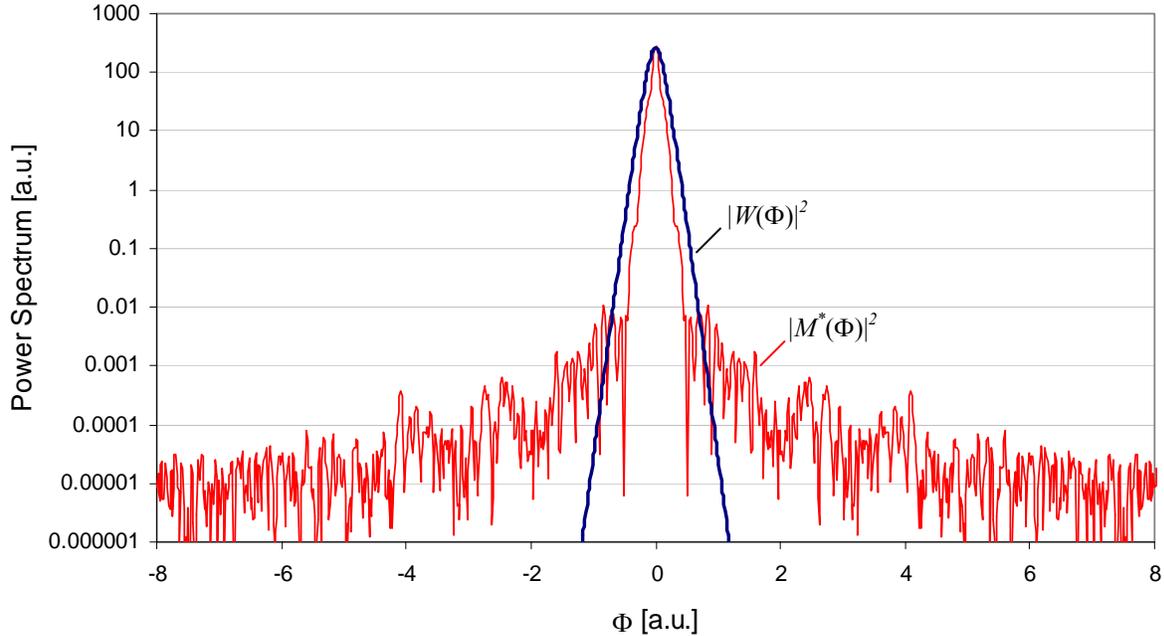

Figure B-1 — Power spectra $|M^*(\Phi)|^2$ and $|W(\Phi)|^2$

It is necessary to apply a filter function $F(\Phi)$ to the quotient $V^*(\Phi) = M^*(\Phi)/W(\Phi)$ prior to the inverse transform.

$$V'(\Phi) = V^*(\Phi) \cdot F(\Phi) = \frac{M^*(\Phi) \cdot F(\Phi)}{W(\Phi)} \tag{B11}$$

The filter should not change the low frequency components of $M^*(\Phi)$, but strongly reduce the high-frequency noise components, i.e., $F(\Phi) \approx 1$ for $|\Phi| < \Phi_0$ and $F(\Phi) \approx 0$ for $|\Phi| > \Phi_0$. The parameter Φ_0 is called the *bandwidth* of the filter.

A possible choice for $F(\Phi)$ which has shown good results in practice is the Fermi-Dirac function

$$F(\Phi) = \left[\exp\left(\frac{|\Phi| - \Phi_0}{\sigma} \right) + 1 \right]^{-1} \tag{B12}$$

The shape of this function is determined by two parameters: the bandwidth Φ_0 and the edge steepness σ (Figure B-2). The larger the bandwidth Φ_0 the better is the resolution of the resulting structure function but the bigger is also the enhancement of higher frequency noise in the signal which can lead to artificial features in the structure function. The influence of the edge steepness σ is more complex: If σ is decreased, the edges of the graph of $F(\Phi)$ become steeper which increases the weight of the signal components with frequencies $\Phi < \Phi_0$ but decreases the weight of the components with frequencies $\Phi > \Phi_0$. Too low values of σ should be avoided since this can also cause artificial steps in the structure function. The parameters have to be adjusted for the best compromise between resolution and noise enhancement; the optimal values depend on the signal-to-noise ratio of the measurement data. $\Phi_0 = 0.45$ and $\sigma = 0.05$ are good values to start with.

Annex B Obtaining time-constant spectra from Z_{th} functions (cont'd)
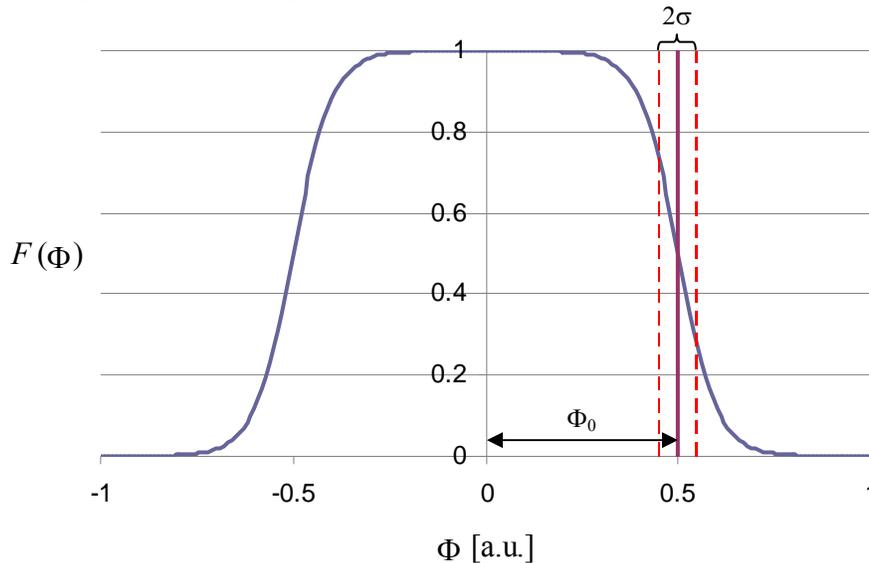
Figure B-2 — Filter function F(Φ)

The steps to compute the time constant spectrum can be summarized as follows:

1. Compute the derivative da/dz of the Z_{th} curve as function of logarithmic time $z = \ln t$

2. Compute the function $w(z)$ according to equation B3

3. Compute the Fourier transforms $M^*(\Phi)$ and $W(\Phi)$ of da/dz and $w(z)$, respectively. The Fast Fourier Transform algorithm should be used to effectively compute the transform.

4. Compute the filter function $F(\Phi)$ according to equation B12 and the quotient

$$V^*(\Phi) = \frac{M^*(\Phi) \cdot F(\Phi)}{W(\Phi)}$$

5. The time constant spectrum $R(z)$ is the inverse Fourier-transform of $V^*(\Phi)$.

Annex C Transformation between FOSTER and CAUER RC network

The targeted network category is the linear passive RC one-ports. Furthermore we restrict our discussion to the case for which

$$Z_{th}(\omega=0) = R_{th} \text{ (a finite value)} \quad \text{and}$$

$$Z_{th}(\omega \to \infty) = 0$$

since these conditions are always true for the thermal impedances.

FOSTER → CAUER transformation. The R_i, C_i element values of the FOSTER model (see Figure C-1a) are assumed to be known. The complex impedance of the network based on the pattern of equation A7 is:

$$\mathbf{Z}(\mathbf{s}) = \sum_{i=1}^{N} \frac{R_i}{1 + \mathbf{s}R_i C_i} \tag{C1}$$

Summing up the members of this expression on a common denominator results in the quotient of two polynomials:

$$\mathbf{Z}(\mathbf{s}) = \frac{n_0 + n_1\mathbf{s} + n_2\mathbf{s}^2 + \ldots + n_{N-1}\mathbf{s}^{N-1}}{d_0 + d_1\mathbf{s} + d_2\mathbf{s}^2 + \ldots + d_N\mathbf{s}^N} \tag{C2}$$

where the n_i, d_i coefficients are of real values.
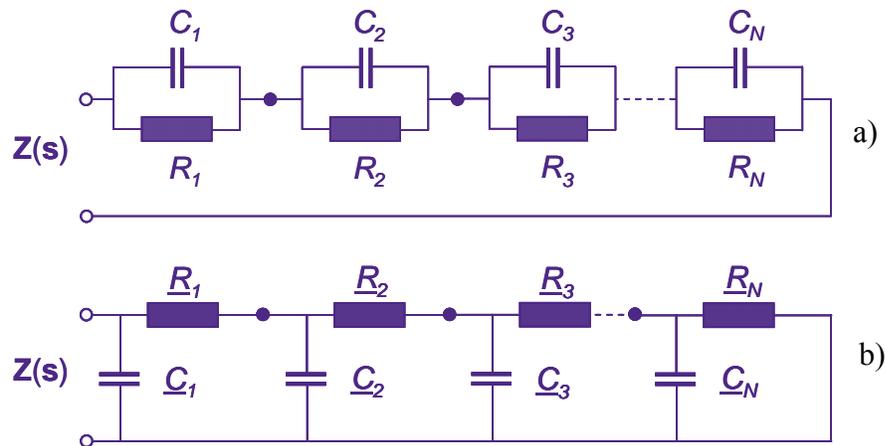

Figure C-1 — Canonical models for RC one-ports. a) FOSTER network, b) CAUER network

In the first step a parallel capacitance will be extracted from $\mathbf{Z}(\mathbf{s})$. If $\mathbf{s} \to \infty$, the admittance can be approximately written as:

$$\mathbf{Y}(\mathbf{s}) = \frac{1}{\mathbf{Z}(\mathbf{s})} \cong \frac{d_N}{n_{N-1}}\mathbf{s} = \underline{C_1}\mathbf{s} \tag{C3}$$

Annex C Transformation between FOSTER and CAUER RC network (cont'd)

The extracted capacitance is $\underline{C_1} = d_N/n_{N-1}$. Now the admittance of this capacitance will be subtracted from $\mathbf{Y(s)} = 1/\mathbf{Z(s)}$. During this subtraction the $\mathbf{s}^N$ element of the numerator vanishes:

$$\mathbf{Y^*(s)} = \mathbf{Y(s)} - \underline{C_1}\mathbf{s} = \frac{d_0 + d_1\mathbf{s} + d_2\mathbf{s^2} + \ldots + d_N\mathbf{s}^N}{n_0 + n_1\mathbf{s} + n_2\mathbf{s^2} + \ldots + n_{N-1}\mathbf{s^{N-1}}} - \underline{C_1}\mathbf{s} = \frac{d_0^* + d_1^*\mathbf{s} + d_2^*\mathbf{s^2} + \ldots + d_{N-1}^*\mathbf{s^{N-1}}}{n_0 + n_1\mathbf{s} + n_2\mathbf{s^2} + \ldots + n_{N-1}\mathbf{s^{N-1}}} \quad \text{(C4)}$$

In the second step a serial resistance will be extracted from $\mathbf{Z^*(s)}$. If $\mathbf{s} \to \infty$, the impedance can be approximately written as:

$$\mathbf{Z^*(s)} \cong \frac{n_{N-1}}{d_{N-11}^*} = \underline{R_1} \quad \text{(C5)}$$

Now this resistance will be subtracted from $\mathbf{Z^*(s)}$. During this subtraction the $\mathbf{s}^{N-1}$ element of the numerator vanishes:

$$\mathbf{Z^{**}(s)} = \mathbf{Z^*(s)} - \underline{R_1} = \frac{n_0 + n_1\mathbf{s} + n_2\mathbf{s^2} + \ldots + n_{N-1}\mathbf{s^{N-1}}}{d_0^* + d_1^*\mathbf{s} + d_2^*\mathbf{s^2} + \ldots + d_{N-1}^*\mathbf{s^{N-1}}} - \underline{R_1} = \frac{n_0^* + n_1^*\mathbf{s} + n_2^*\mathbf{s^2} + \ldots + n_{N-2}^*\mathbf{s^{N-2}}}{d_0^* + d_1^*\mathbf{s} + d_2^*\mathbf{s^2} + \ldots + d_{N-1}^*\mathbf{s^{N-1}}} \quad \text{(C6)}$$

Now we have again an impedance formula like equation B2 but the order of both the numerator and the denominator have been reduced by 1. By applying successively the above procedure the further $\underline{C_2}$, $\underline{R_2}$ etc. elements of the ladder network shown in Figure B-1b can be calculated. This procedure has to be continued until $\mathbf{Z}=0$ reached.

CAUER → FOSTER transformation. The $\underline{R_i}$, $\underline{C_i}$ element values of the CAUER model (see Figure C-1b) are assumed to be known. The complex impedance of the network is:

$$\mathbf{Z(s)} = \cfrac{1}{\mathbf{s}\underline{C_1} + \cfrac{1}{\underline{R_1} + \cfrac{1}{\mathbf{s}\underline{C_2} + \cfrac{1}{\underline{R_2} + \ldots}}}} \quad \text{(C7)}$$

This expression can be transformed to the form of equation C2 by elementary steps. Thereafter the N roots of the denominator have to be calculated. These $\mathbf{s}_i$ roots are of negative real values each and determine the R_iC_i time-constants of the system: $R_iC_i = 1/|\mathbf{s}_i|$.

The R_i values can be calculated by

$$R_i = \left. \frac{n_0 + n_1\mathbf{s} + n_2\mathbf{s^2} + \ldots + n_{N-1}\mathbf{s^{N-1}}}{\dfrac{d}{d\mathbf{s}}\left(d_0 + d_1\mathbf{s} + d_2\mathbf{s^2} + \ldots + d_N\mathbf{s}^N\right)} \right|_{\mathbf{s}=\mathbf{s_i}} \quad \text{(C8)}$$

Annex C Transformation between FOSTER and CAUER RC network (cont'd)

A practical problem has still to be discussed. In order to reach good resolution on the structure function a reasonably high number of Δz sections should be applied during the discretization of the $R(z)$ function. The number of RC stages shown in Figure A-9 in Annex A may reach the 100 or 200. The algorithm of the FOSTER$\rightarrow$CAUER transformation holds numerical problems for such big circuits.

Both the range and the length of the mantissa have to be extended in the representation of the floating numbers. Usually even the 'long double' (usually 10 bytes) representation is not accurate enough. An extended precision arithmetic has to be used as provided for example by the GNU Multiple Precision Arithmetic Library (http://gmplib.org/).

Annex D (normative) Transient Dual Interface Measurement Evaluation Software Benchmark

The following transient dual interface measurement examples are provided along with this document to serve as a benchmark. Any implementation of the evaluation algorithms described herein should reproduce the θ_{JC} values for these measurements within the given tolerances.

Measurement	Description	Evaluation method	θ_{JC}
MOSFET_dry MOSFET_tim	MOSFET device in PG-TO-263-3 package. *Solder die attach*.	Point of separation of $Z_{\theta JC}$ curves (*method 1*)	(0.27 ± 0.04) K/W
HBRIDGE_dry HBRIDGE_tim	H-Bridge switch in PG-DSO-20 exposed die pad package. *Glue die attach*.	Point of separation of the structure functions (*method 2*)	(3.6 ± 0.3) K/W

_dry refers to dry measurement without thermal grease.
_tim refers to measurement with thermal grease.

JEDEC

STANDARD IMPROVEMENT FORM   **JEDEC   JESD51-14**

The purpose of this form is to provide the Technical Committees of JEDEC with input from the industry regarding usage of the subject standard. Individuals or companies are invited to submit comments to JEDEC. All comments will be collected and dispersed to the appropriate committee(s).

If you can provide input, please complete this form and return to:

JEDEC   Fax: 703.907.7583
Attn: Publications Department
3103 North 10th Street
Suite 240 South
Arlington, VA 22201-2107

---

1.   I recommend changes to the following:
    ☐   Requirement, clause number _____

    ☐   Test method number _____   Clause number _____

    The referenced clause number has proven to be:
    ☐ Unclear   ☐   Too Rigid   ☐   In Error

    ☐   Other _____

---

2.   Recommendations for correction:

    _____

    _____

    _____

    _____

---

3.   Other suggestions for document improvement:

    _____

    _____

    _____

    _____

Submitted by

Name: _____   Phone: _____

Company: _____   E-mail: _____

Address: _____

City/State/Zip: _____   Date: _____